

<sup>1</sup> Increasing prevalence of plant-fungal symbiosis across two  
<sup>2</sup> centuries of environmental change

<sup>3</sup> Joshua C. Fowler<sup>1,2\*</sup>

Jacob Moutouama<sup>1</sup>

Tom E. X. Miller<sup>1</sup>

<sup>4</sup> 1. Rice University, Department of BioSciences, Houston, Texas 77006; 2. University of Miami,  
<sup>5</sup> Department of Biology, Miami, Florida;  
<sup>6</sup> \* Corresponding author; e-mail: jcf221@miami.edu.

<sup>7</sup> *Manuscript elements:* Figure 1 - Figure 5, Appendix A (including Figure A1 - Figure A14, Table  
<sup>8</sup> A1, and Supplemental Methods).

<sup>9</sup> *Keywords:* climate change, plant-microbe symbiosis, herbarium, museum specimen, spatially-  
<sup>10</sup> varying coefficients model, *Epichloë*, *Poaceae*.

<sup>11</sup> *Manuscript type:* Research Article.

<sup>12</sup> Prepared using the suggested L<sup>A</sup>T<sub>E</sub>X template for *Am. Nat.*

## Abstract

14 Species' distributions and abundances are shifting in response to ongoing global climate change.  
15 Mutualistic microbial symbionts can provide their hosts with protection from environmental  
16 stress that may contribute towards resilient responses to environmental change, however these  
17 changes may also disrupt species interactions and lead to declines in hosts and/or symbionts.  
18 Symbionts preserved within natural history specimens offer a unique opportunity to quantify  
19 changes in microbial symbiosis across broad temporal and spatial scales. We asked how the  
20 prevalence of seed-transmitted fungal symbionts of grasses (*Epichloë* endophytes) have changed  
21 over time in response to climate change, and how these changes vary across host species' ranges.  
22 Specifically, we analyzed 2,346 herbarium specimens of three grass host species (*Agrostis hye-*  
23 *malis*, *Agrostis perennans*, *Elymus virginicus*) collected over the past two centuries (1824 – 2019) for  
24 the presence or absence of *Epichloë* symbiosis. We found that endophytes increased in preva-  
25 lence over the last two centuries from ca. 25% prevalence to ca. 75% prevalence, on average,  
26 across three host species. Changes in seasonal climate drivers were associated with increasing  
27 endophyte prevalence. Notably, increasing precipitation during the peak growing season for  
28 *Agrostis* species and decreasing precipitation for *E. virginicus* were associated with increasing en-  
29 dophyte prevalence. Changes in the variability of precipitation and temperature during off-peak  
30 seasons were also important predictors of increasing endophyte prevalence. Our analysis per-  
31 formed favorably in an out-of-sample predictive test with contemporary survey data, a rare extra  
32 step in collections-based research. However, we identified greater local-scale variability in endo-  
33 phyte prevalence in contemporary data compared to model predictions based on historic data,  
34 suggesting new directions that could improve predictive accuracy. Our results provide novel  
35 evidence for a cryptic biological response to climate change that may contribute to the resilience  
36 of host-microbe symbiosis through context-dependent benefits that confer a fitness advantage to  
37 symbiotic hosts under environmental change.

38 Abstract : 300 words

## Introduction

40 Understanding how biotic interactions are altered by global change is a major goal of basic and  
41 applied ecological research (Blois et al., 2013; Gilman et al., 2010). Documented responses to  
42 environmental change, such as shifts in species' distributions (Aitken et al., 2008) and phenology  
43 (Piao et al., 2019), are typically blind to concurrent changes in associated biotic interactions.  
44 Empirically evaluating these biotic changes – whether interacting species shift in tandem with  
45 their partners or not (HilleRisLambers et al., 2013) – is crucial to predicting the reorganization  
46 of Earth's biodiversity under global change. Such evaluations have been limited because few  
47 datasets on species interactions extend over sufficiently long time scales of contemporary climate  
48 change (Poisot et al., 2021).

49 Natural history specimens, which were originally collected to study and preserve taxonomic  
50 diversity, present a unique opportunity to explore long-term changes in ecological interactions  
51 across broad spatial and temporal scales (Meineke et al., 2018). Natural history collections, built  
52 and maintained by the efforts of thousands of scientists, are invaluable time machines, primarily  
53 comprised of physical specimens of organisms along with information about the time and place  
54 of their collection. These specimens often preserve physical legacies of ecological processes and  
55 species' interactions from dynamically changing environments across time and space. For exam-  
56 ple, previous researchers have used plant collections (herbaria) to document shifts in phenology  
57 (Berg et al., 2019; Park et al., 2019; Willis et al., 2017), pollination (Duan et al., 2019; Pauw and  
58 Hawkins, 2011), and herbivory (Meineke et al., 2019) related to anthropogenic climate change.  
59 However, few previous studies have leveraged biological collections to examine climate change-  
60 related shifts in a particularly common type of interaction: microbial symbiosis.

61 Microbial symbionts are common to all macroscopic organisms and can have important ef-  
62 fects on their hosts' survival, growth and reproduction (McFall-Ngai et al., 2013; Rodriguez et al.,  
63 2009). Many microbial symbionts act as mutualists, engaging in reciprocally beneficial interac-  
64 tions with their hosts that can ameliorate environmental stress. For example, bacterial symbionts

65 of insects, such as *Wolbachia*, can improve their hosts' thermal tolerance (Renoz et al., 2019; Truitt  
66 et al., 2019), and arbuscular mycorrhizal fungi, documented in 70-90% of families of land plants  
67 (Parniske, 2008), allow their hosts to persist through drought conditions by improving water and  
68 nutrient uptake (Cheng et al., 2021). On the other hand, changes in the mean and variance of  
69 environmental conditions may disrupt microbial mutualisms by changing the costs and bene-  
70 fits of the interaction for each partner, leading the interaction to deteriorate (Aslan et al., 2013;  
71 Fowler et al., 2024). Coral bleaching (the loss of symbiotic algae) due to temperature stress (Sully  
72 et al., 2019) is perhaps the best known example, but this phenomenon is not unique to corals.  
73 Lichens exposed to elevated temperatures experienced loss of photosynthetic function along with  
74 changes in the composition of their algal symbiont community (Meyer et al., 2022). How com-  
75 monly and under what conditions microbial mutualisms deteriorate or strengthen under climate  
76 change remain unanswered questions (Frederickson, 2017). Previous work suggests that these  
77 alternative responses may depend on the intimacy and specialization of the interaction as well  
78 as the physiological tolerances of the mutualist partners (Rafferty et al., 2015; Toby Kiers et al.,  
79 2010; Warren and Bradford, 2014).

80 Understanding of how microbial symbioses are affected by climate change is additionally  
81 complicated by spatial heterogeneity in the direction and magnitude of environmental change  
82 (IPCC, 2021). Beneficial symbionts are likely able to shield their hosts from environmental stress  
83 in locations that experience a small degree of change, but symbionts in locations that experience  
84 changes of large magnitude may be pushed beyond their physiological limits (Webster et al.,  
85 2008). Additionally, symbionts are often unevenly distributed across their hosts' distribution.  
86 Facultative symbionts may be absent from portions of the host range (Afkhami et al., 2014), and  
87 hosts may engage with a diversity of partners (different symbiont species or locally-adapted  
88 strains) across their environments (Fowler et al., 2023; Fraude et al., 2008; Rolshausen et al., 2018).  
89 Identifying broader spatial trends in symbiont prevalence is therefore an important step in de-  
90 veloping predictions for where to expect changes in the symbiosis in future climates.

91 *Epichloë* fungal endophytes are specialized symbionts of cool-season grasses, which have been

92 documented in ~ 30% of cool-season grass species (Leuchtmann, 1992). They are transmitted  
93 vertically from maternal plants to offspring through seeds. Vertical transmission creates a feed-  
94 back between the fitness of host and symbiont (Douglas, 1998; Fine, 1975; Rudgers et al., 2009).  
95 Over time, endophytes that act as mutualists should rise in prevalence within a host population  
96 (Donald et al., 2021). *Epichloë* are known to improve their hosts' drought tolerance (Decunta  
97 et al., 2021) and protect their hosts against herbivores (Crawford et al., 2010) and pathogens (Xia  
98 et al., 2018) likely through the production of a diverse suite of alkaloids and other secondary  
99 metabolites. The fitness feedback induced by vertical transmission leads to the prediction that  
100 endophyte prevalence should be high in populations where these fitness benefits are most impor-  
101 tant. Previous survey studies of contemporary populations have documented large-scale spatial  
102 patterns in endophyte prevalence structured by environmental gradients (Afkhami, 2012; Bazely  
103 et al., 2007; Granath et al., 2007; Sneck et al., 2017). We predicted that prevalence should track  
104 temporal changes in environmental drivers that elicit strong fitness benefits.

105 Early research on *Epichloë* used herbarium specimens to describe the broad taxonomic di-  
106 versity of host species that harbor these symbionts (White and Cole, 1985), establishing that  
107 endophyte symbiosis could be identified in plant tissue from as early as 1851. However, no  
108 subsequent studies, to our knowledge, have used the vast resources of biological collections to  
109 quantitatively assess spatio-temporal trends in endophyte prevalence and their environmental  
110 correlates. Grasses are commonly collected and identified based on the presence of their re-  
111 productive structures, meaning that preserved specimens typically contain seeds, conveniently  
112 preserving the fungi along with their host plants on herbarium sheets. This creates the oppor-  
113 tunity to leverage the unique spatio-temporal sampling of herbarium collections to examine the  
114 response of the symbiosis to historical climate change. However, the predictive ability derived  
115 from historical analyses is rarely tested against contemporary data (Lee et al., 2024). Critically  
116 evaluating whether insights from historical reconstruction are predictive of variation across con-  
117 temporary populations is a crucial step for the field to move from reading signatures of the past  
118 to forecasting ecological dynamics into the future.

119 In this study, we assessed the long-term responses of endophyte symbiosis to climate change  
120 through the use of herbarium specimens of three North American host grass species (*Agrostis*  
121 *hyemalis*, *Agrostis perennans*, and *Elymus virginicus*). We first addressed questions describing spa-  
122 tial and temporal trends in endophyte prevalence: (i) How has endophyte prevalence changed  
123 over the past two centuries? and (ii) How spatially variable are temporal trends in endophyte  
124 prevalence across eastern North America? We then addressed how climate change may be driv-  
125 ing trends in endophyte prevalence by asking: (iii) What is the relationship between temporal  
126 trends in endophyte prevalence and associated changes in climate drivers? We predicted that  
127 aggregate endophyte prevalence would increase over time in tandem with climate warming, and  
128 that hotspots of endophyte change would correspond spatially to hotspots of climate change.  
129 Finally, we evaluated the performance of models built on data from historic specimens with an  
130 out-of-sample test, using data on endophyte prevalence from contemporary surveys of host pop-  
131 ulations. To answer these questions we examined a total of 2,346 historic specimens collected  
132 across eastern North America between 1824 and 2019, and evaluated model performance against  
133 contemporary surveys comprising 1,442 individuals from 63 populations collected between 2013  
134 and 2020.

## 135 Methods

### 136 Focal species

137 Our surveys focused on three native North American grasses: *Agrostis hyemalis*, *Agrostis peren-*  
138 *nans*, and *Elymus virginicus*. Both *Agrostis* species host *Epichloë amarillans* (Craven et al., 2001;  
139 Leuchtmann et al., 2014), while *Elymus virginicus* typically hosts *Epichloë elymi* (Clay and Schardl,  
140 2002). These C<sub>3</sub> grass species are commonly represented in natural history collections with broad  
141 distributions covering much the eastern United States (Fig. 1). *A. hyemalis* is a small short-lived  
142 perennial species that germinates in spring and typically flowers between March and July (most  
143 common collection month: May). *A. perennans* is of similar stature but is longer lived than

<sup>144</sup> *Agrostis hyemalis* and flowers in late summer and early autumn (most common collection month:  
<sup>145</sup> September). *A. perennans* is more sparsely distributed, tending to be found in shadier and more  
<sup>146</sup> moist habitats, while *A. hyemalis* is commonly found in open and recently disturbed ground.  
<sup>147</sup> Both *Agrostis* species are recorded from throughout the Eastern US, but *A. perennans* has a slightly  
<sup>148</sup> more northern distribution, whereas *A. hyemalis* is found rarely as far north as Canada and is  
<sup>149</sup> listed as a rare plant in Minnesota. *E. virginicus* is a larger and relatively longer-lived species that  
<sup>150</sup> is more broadly distributed than the *Agrostis* species. It begins flowering as early as March or  
<sup>151</sup> April but continues throughout the summer (most common collection month: July).

<sup>152</sup> *Herbarium surveys*

<sup>153</sup> We visited nine herbaria between 2019 and 2022 (see Table A1 for a summary of specimens in-  
<sup>154</sup> cluded from each collection). With permission from herbarium staff, we acquired seed samples  
<sup>155</sup> from 1135 *A. hyemalis* specimens collected between 1824 and 2019, 357 *A. perennans* specimens  
<sup>156</sup> collected between 1863 and 2017, and 854 *E. virginicus* specimens collected between 1839 and  
<sup>157</sup> 2019 (Fig. 1, Fig. 2A, Fig. A1). We chose our focal species in part because they are commonly  
<sup>158</sup> represented in herbarium collections, and produce high numbers of seeds, meaning that small  
<sup>159</sup> samples would not diminish the value of the specimens for future studies. We collected up  
<sup>160</sup> to 5-10 seeds per specimen after examining the herbarium sheet under a dissecting microscope  
<sup>161</sup> to ensure that we collected mature seeds, not florets or unfilled seeds, fit for our purpose of  
<sup>162</sup> identifying fungal endophytes with microscopy. We excluded specimens for which information  
<sup>163</sup> about the collection location and date were unavailable. Each specimen was assigned geographic  
<sup>164</sup> coordinates based on collection information recorded on the herbarium sheet using the geocod-  
<sup>165</sup> ing functionality of the ggmap R package (Kahle et al., 2019). Many specimens had digitized  
<sup>166</sup> collection information readily available, but for those that did not, we transcribed information  
<sup>167</sup> printed on the herbarium sheet. Collections were geo-referenced to the nearest county centroid,  
<sup>168</sup> or nearest municipality when that information was available. For fifteen of the oldest specimens,  
<sup>169</sup> only information at the state level was available, and so we used the state centroid.

170 After collecting seed samples, we quantified the presence or absence of *Epichloë* fungal hyphae  
171 in each specimen using microscopy. We first softened seeds with a 10% NaOH solution, then  
172 stained the seeds with aniline blue-lactic acid stain and squashed them under a microscope  
173 cover slip. We examined the squashed seeds for the presence of fungal hyphae at 200-400X  
174 magnification (Bacon and White, 2018). On average we scored 4.7 intact seeds per specimen of  
175 *A. hyemalis*, 4.2 seeds per specimen of *A. perennans*, and 3.8 seeds per specimen of *E. virginicus*;  
176 we scored 10,342 seeds in total. . Due to imperfect vertical transmission (Afkhami and Rudgers,  
177 2008), it is possible that symbiotic host-plants produce a mixture of symbiotic and non-symbiotic  
178 seeds. We therefore designated a specimen as endophyte-symbiotic if *Epichloë* hyphae were  
179 observed in one or more of its seeds, or non-symbiotic if *Epichloë* hyphae were observed in none  
180 of its seeds. To capture uncertainty in the endophyte scoring process, we recorded both a "liberal"  
181 and a "conservative" endophyte status for each plant specimen. When we identified potential  
182 endophytes with unusual morphology, low uptake of stain, or a small amount of fungal hyphae  
183 across the scored seeds, we recorded a positive liberal status (more likely to be endophyte-  
184 positive) and a negative conservative status (less likely to be endophyte-positive). 89% of scored  
185 plants had matching liberal and conservative scores, reflecting high confidence in endophyte  
186 status. The following analyses used the liberal status, but we repeated all analyses with the  
187 conservative status which yielded qualitatively similar results (Fig. A8).

### 188 *Modeling spatial and temporal changes in endophyte prevalence*

189 We assessed spatial and temporal changes in endophyte prevalence across each host distribution,  
190 quantifying the "global" temporal trends aggregated across space, and then examining spatial  
191 heterogeneity in the direction and magnitude of endophyte change (hotspots and coldspots)  
192 across the spatial extent of each host's distribution. To account for the spatial non-independence  
193 of geo-referenced occurrences, we used an approximate Bayesian method, Integrated Nested  
194 Laplace Approximation (INLA), to construct spatio-temporal models of endophyte prevalence.  
195 INLA provides a computationally efficient method of ascertaining parameter posterior distribu-

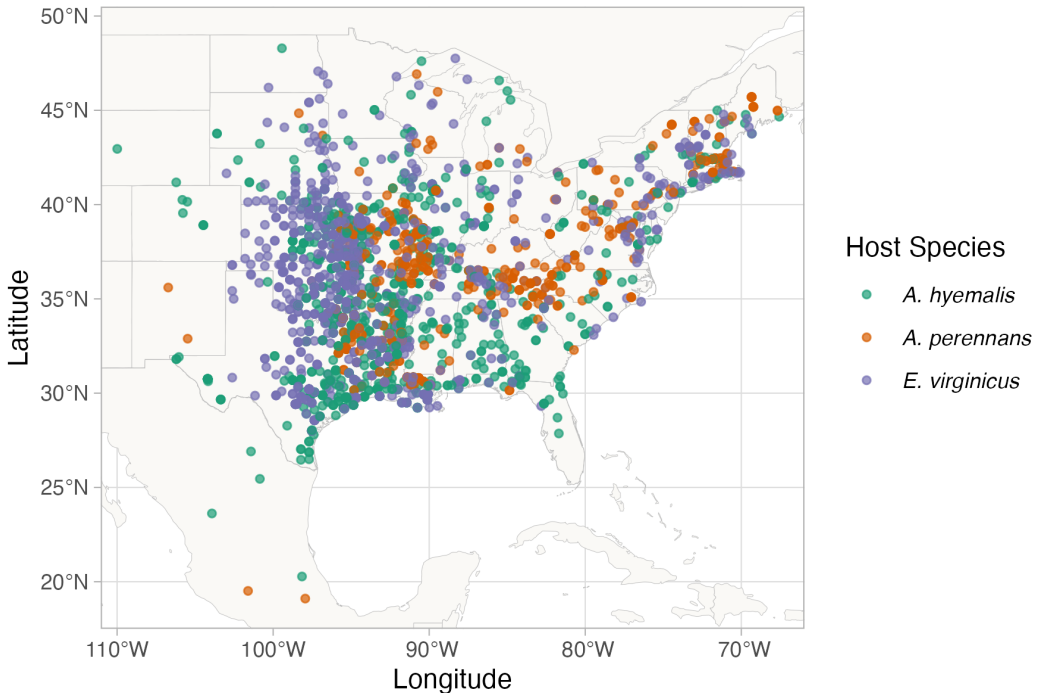


**Figure 1: Collection locations of herbarium specimens sampled for *Epichloë* endophytes.** Specimens span eastern North America from nine herbaria, and are colored by host species.

196 tions for certain models that can be formulated as latent Gaussian Models (Rue et al., 2009).  
 197 Many common statistical models, including structured and unstructured mixed-effects models,  
 198 can be represented as latent Gaussian Models. We incorporated spatial heterogeneity into this  
 199 analysis using spatially-structured intercept and slope parameters implemented as stochastic  
 200 partial differential equations (SPDE) to approximate a continuous spatial Gaussian process. This  
 201 SPDE approach is a flexible method of smoothing across space while explicitly accounting for  
 202 spatial dependence between data-points (Bakka et al., 2018; Lindgren et al., 2011). Fitting models  
 203 with structured spatial effects is possible with MCMC sampling but can require long computa-  
 204 tion times, making INLA an effective alternative. This approach has been used to model spatial  
 205 patterns in flowering phenology (Willems et al., 2022), the abundance of birds (Meehan et al.,  
 206 2019) and butterflies (Crossley et al., 2022), the distribution of temperate trees (Engel et al., 2022)  
 207 as well as the population dynamics of endangered amphibians (Knapp et al., 2016) and other

208 ecological processes (Beguin et al., 2012).

209 We estimated global and spatially-varying trends in endophyte prevalence using a joint-  
210 likelihood model. For each host species  $h$ , endophyte presence/absence of the  $i^{th}$  specimen ( $P_{h,i}$ )  
211 was modeled as a Bernoulli response variable with expected probability of endophyte occurrence  
212  $\hat{P}_{h,i}$ . We modeled  $\hat{P}_{h,i}$  as a linear function of intercept  $A_h$  and slope  $T_h$  defining the global trend  
213 in endophyte prevalence specific to each host species as well as with spatially-varying intercepts  
214  $\alpha_{h,l_i}$  and slopes  $\tau_{h,l_i}$  associated with location ( $l_i$ , the unique latitude-longitude combination of the  
215  $i^{th}$  observation). The joint-model structure allowed us to “borrow strength” across species in  
216 the estimation of shared variance terms for the spatially-dependent random effect  $\delta_{l_i}$ , intended  
217 to account for residual spatial variation, and  $\chi_{c_i}$  and  $\omega_{s_i}$  i.i.d.-random effects indexed for each  
218 collector identity ( $c_i$ ), and scorer identity ( $s_i$ ) of the  $i^{th}$  specimen.

$$\text{logit}(\hat{P}_{h,i}) = A_h + T_h * \text{year}_i + \alpha_{h,l_i} + \tau_{h,l_i} * \text{year}_i + \delta_{l_i} + \chi_{c_i} + \omega_{s_i} \quad (1)$$

219 By including random effects for collectors and scorers, we accounted for “nuisance” variance  
220 that may bias predictions for changes in endophyte prevalence. Previous work suggests that  
221 behavior of historical botanists may introduce biases into ecological inferences made from historic  
222 collections (Kozlov et al., 2020). Prolific collectors who contribute thousands of specimens may  
223 be more or less likely to collect certain species, or specimens with certain traits (Daru et al., 2018).  
224 Similarly, the process of scoring seeds for hyphae involved several student researchers who, even  
225 with standardized training, may vary in their likelihood of positively identifying *Epichloë*.

226 We performed model fitting using the inlabru R package (Bachl et al., 2019). Global intercept  
227 and slope parameters  $A$ , and  $T$ , were given vague priors. Scorer and collector random effects,  
228  $\chi$  and  $\omega$ , were given penalized complexity priors, with distributions approximating a Normal  
229 distribution with standard deviation of 5. Each spatially-structured parameter depended on a  
230 covariance matrix according to the proximity of each pair of collection locations (Bakka et al.,  
231 2018; Lindgren et al., 2011). The covariance matrix was approximated using a Matérn covariance  
232 function, with each data point assigned a location according to the nodes of a mesh of non-

233 overlapping triangles encompassing the study area (Fig. A2). We assessed model fit with visual  
234 posterior predictive checks (A3) and measurements of AUC (Figs. A4-A5). Priors for the Matérn  
235 covariance function, termed "range" and "variance", define how proximity effects decay with  
236 distance. Results presented in the main text reflect a prior range of 342 kilometers (i.e. a 50%  
237 probability of estimating a range less than 342 kilometers). We tested a range of values (from 68  
238 kilometers to 1714 kilometers) and meshes (presented in the Supporting Methods), finding that  
239 while the magnitude and uncertainty of effects varied, model results were qualitatively similar,  
240 i.e. the same direction of effects across space.

241 *Modeling distributions of host species*

242 Because the herbarium records did not encompass the entirety of these host species' ranges,  
243 we additionally modeled the geographic distribution of each host species to generate realistic  
244 maps on which we could project the predictions of the INLA model. We followed the ODMAP  
245 (overview, data, model, assessment, prediction) protocol (Crossley et al., 2022) (see Supporting  
246 Methods). In short, we used presence-only observations of each host species from Global Bio-  
247 diversity Information Facility (GBIF) between 1990 to 2020. We fit maximum entropy (MaxEnt)  
248 models using the maxent function in the R package dismo (Hijmans et al., 2017) using the same  
249 set of seasonal climate predictors considered above calculated for the 1990-2020 climate normals:  
250 mean and standard deviation of spring, summer, and autumn temperature, and mean and stan-  
251 dard deviation of spring, summer, and autumn cumulative precipitation. We generated 10,000  
252 pseudo-absences as background points, and split the occurrence data into 75% for model train-  
253 ing and 25% for model testing. The performance of models was evaluated with AUC (Jiménez-  
254 Valverde, 2012). We found AUC values of 0.862, 0.838, 0.821 respectively for *Agrostis hyemalis*,  
255 *Agrostis perennans*, and *Elymus virginicus* indicating good model fit to data. To convert the contin-  
256 uous predicted probabilities into binary presence - absence maps on which we projected INLA  
257 predictions, we used the training sensitivity (true positive rate) and specificity threshold (true  
258 negative rate) (Liu et al., 2005).

259

## Assessing the role of climate drivers

260 We assessed how the magnitude of climate change may have driven changes in endophyte preva-  
261 lence by assessing correlations between changes in climate and changes in endophyte prevalence  
262 predicted from our spatial model at evenly spaced pixels across the study area. We first down-  
263 loaded monthly temperature and precipitation rasters from the PRISM climate group (Daly and  
264 Bryant, 2013) covering the time period between 1895 and 2020 using the 'prism' R package (Hart  
265 and Bell, 2015). Prism provides reconstructions of historic climate variables across the United  
266 States by spatially-interpolating weather station data (Di Luzio et al., 2008). We calculated 30-year  
267 climate normals for seasonal mean temperature and cumulative precipitation for the recent (1990  
268 to 2020) and historic (1895 to 1925) periods. We used three four-month seasons within the year  
269 (Spring: January, February, March, April; Summer: May, June, July, August; Autumn: September,  
270 October, November, December). This division of seasons allowed us to quantify differences in  
271 climate associated with the two "cool" seasons, when we expected our focal species to be most  
272 biologically active (*A. hyemalis* flowering phenology: spring; *E. virginicus*: spring and summer; *A.*  
273 *perennans*: autumn). In addition to mean climate conditions, environmental variability itself can  
274 influence population dynamics (Tuljapurkar, 1982) and changes in variability are a key prediction  
275 of climate change models (IPCC, 2021; Stocker et al., 2013). Therefore, we calculated the standard  
276 deviation for each annual and seasonal climate driver across each 30-year period. We then took  
277 the difference between recent and historic periods for the mean and standard deviation for each  
278 climate driver (Figs. A12-A14). All together, we assessed twelve potential climate drivers: the  
279 mean and standard deviation of spring, summer, and autumn temperature, as well as the mean  
280 and standard deviation of spring, summer, and autumn cumulative precipitation.

281 To evaluate whether areas that have experienced the greatest changes in endophyte preva-  
282 lence (hotspots of endophyte change) are associated with high degrees of change in climate  
283 (hotspots of climate change), we modeled the fitted, spatially-varying slopes of endophyte change  
284 through time ( $\tau_{[h]l}$  as a linear function of environmental covariates, with a Gaussian error distri-

bution. Data from each host species was analyzed separately. Fitting regressions to many pixels across the study region risks artificially inflating confidence in our results due to large sample sizes, and so we performed this analysis using only a random subsample of 250 pixels across the study region; other sizes of subsample yielded similar results.

*Validating model performance with in-sample and out-of-sample tests*

We evaluated the predictive ability of the model using both in-sample training data from the herbarium surveys, and with out-of-sample test data, an important but rarely used strategy in ecological studies (Lee et al., 2024; Tredennick et al., 2021). We generated out-of-sample test data from contemporary surveys of endophyte prevalence in natural populations of *A. hyemalis* and *E. virginicus* in Texas and the southern US. Surveys of *E. virginicus* were conducted in 2013 as described in Sneck et al. (2017), and surveys of *A. hyemalis* took place between 2015 and 2020. Population surveys of *A. hyemalis* were initially designed to cover longitudinal variation in endophyte prevalence towards its range edge, while surveys of *E. virginicus* were designed to cover latitudinal variation. In total, we visited 43 populations of *A. hyemalis* and 20 populations of *E. virginicus* across the south-central US, with emphasis on Texas and neighboring states (Fig A11). During surveys, we collected seeds from up to 30 individuals per population (average number of plants sampled per population: 22.9); note that this sampling design provided greater local depth of information than the herbarium records, where only one plant was sampled at each locality. We quantified the endophyte status of each individual with staining microscopy as described for the herbarium surveys (with 5-10 seeds scored per individual), and calculated the prevalence of endophytes within the population (proportion of plants that were endophyte-symbiotic). For each population, we compared the observed fraction of endophyte-symbiotic hosts to the predicted probability of endophyte occurrence  $\hat{P}$  derived from the model for that location and year. The contemporary survey period (2013-2020) is at the most recent edge of the time period encompassed by the historical observations used for model fitting.

310

## Results

### 311 *How has endophyte prevalence changed over time?*

312 Across >2300 herbarium specimens dating back to 1824, we found that prevalence of *Epichloë*  
313 endophytes increased over the last two centuries for all three grass host species (Fig. 2). On  
314 average, endophytes of *A. perennans* and *E. virginicus* increased from ~ 40 % to 70% prevalence  
315 across the study region, and *A. hyemalis* increased from ~ 25% to over 50% prevalence. Our  
316 model indicates a high certainty that overall temporal trends are positive across species (99%  
317 probability of a positive overall year slope in *A. hyemalis*, 92% probability of a positive overall  
318 year slope in *A. perennans*, and 91% probability of a positive overall year slope in *E. virginicus*)  
319 (Fig. A6).

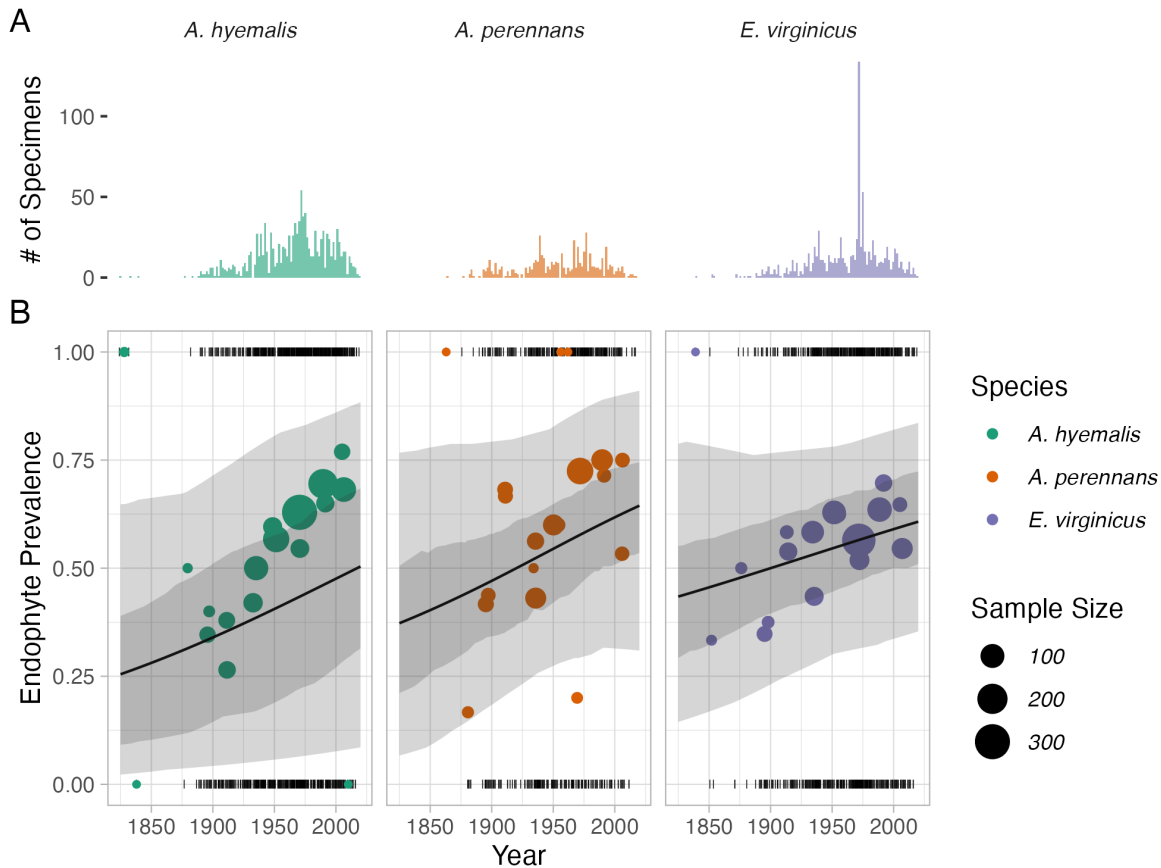


Figure 2: **Temporal trends in endophyte prevalence.** (A) Histograms show the frequency of scored specimens through time for each host species. (B) Lines show predicted mean endophyte prevalence over the study period along with the 50% and 95% CI bands incorporating uncertainty associated with collector and scorer random effects. Colored points are binned means of the observed endophyte presence/absence data (black dashes). Colors represent each host species and point size represents the number of specimens.

320        The model appears to under-predict the observed increase in endophyte prevalence relative  
 321        to the data, particularly for *A. hyemalis* (Fig. 2B), but the model is accounting for random effects  
 322        and spatial non-independence that are not readily seen in the figure. We found no evidence that  
 323        collector biases influenced our results. Collector random effects were consistently small (Fig.  
 324        A9), and models fit with and without this random effect provide qualitatively similar results.

325 The identity of individual scorers did contribute to observed patterns in endophyte prevalence.  
326 For example, 3 of the 25 scorers were more consistently likely than average to assign positive  
327 endophyte status, as indicated by 95% credible intervals greater than zero (Fig. A10). It is  
328 difficult to distinguish whether this was driven by true differences in scorers biases during the  
329 seed scoring process or by unintended spatial or temporal clustering of the specimens scored by  
330 each scorer (Clayton et al., 1993; Urdangarin et al., 2023). By under-weighting endophyte-positive  
331 samples that are clustered spatially or by collector or observer, the INLA model is appropriately  
332 accounting for nuisance variables and providing a conservative inference of endophyte change  
333 relative to the raw data.

334 *How spatially variable are temporal trends in endophyte prevalence?*

335 While there was an overall increase in endophyte prevalence, our model revealed hotspots and  
336 coldspots of change across the host species' ranges, which are mapped in Fig. 3 across geo-  
337 graphic ranges predicted by MaxEnt species distribution models. In some regions, posterior  
338 mean estimates of spatially varying temporal trends indicate that *A. hyemalis* and *A. perennans*  
339 experienced increases in prevalence by as much as 2% per year over the study period, while  
340 *E. virginicus* experienced increases up to around 1% per year. Both *Agrostis* species show areas  
341 of strong increase and areas of declining prevalence, while *E. virginicus* had an overall weaker  
342 and geographically more homogeneous increase in endophyte prevalence. Notably, endophytes  
343 increased most strongly towards the western range edge of *A. hyemalis* (Fig. 3A) and across the  
344 northeastern US for *A. perennans* (Fig. 3B). Posterior estimates of uncertainty in spatially varying  
345 slopes indicate that these hotspots of change may have experienced increases of up to 5% per  
346 year while declines in prevalence may be as great as 4% per year for *A. hyemalis* and *A. perennans*.  
347 For *E. virginicus*, uncertainty ranges between 3.5% increases and 2.5% decreases (Fig. A7).

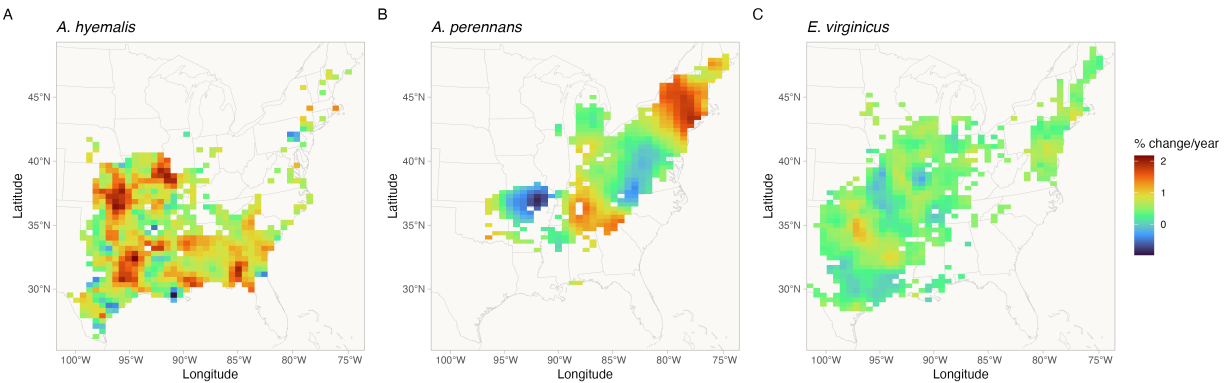


Figure 3: Predicted posterior mean of spatially-varying slopes representing change in endophyte prevalence for each host species. Color indicates the relative change in predicted endophyte prevalence.

*What is the relationship between variation in temporal trends in endophyte prevalence and changes in climate drivers?*

We found that trends in endophyte prevalence were strongly associated with seasonal climate change drivers (Fig. 4). For the majority of the study region, the climate has become wetter (an average increase in annual precipitation of 60 mm.) with relatively little temperature warming (an average increase in annual temperature of 0.02 °C) over the last century (Fig. A12-A14), a consequence of regional variation in global climate change (IPCC, 2021). Within the region, climate changes were spatially variable; certain locations experienced increases in annual precipitation as large as 375 mm. or decreases up to 54 mm. across the last century, while annual temperature changes ranged from warming as great as 1.4 °C to cooling by 0.46 °C. Spatially variable climate trends were predictive of trends in endophyte prevalence. For example, strong increases in endophyte prevalence for *A. perennans* were most strongly associated with increasing autumn precipitation and with increasing mean and variability in autumn temperature (greater than 97% posterior probabilities of positive slopes). For this species, a 1 °C increase in autumn temper-

ature was associated with a 1.07 % increase per year in endophyte prevalence (Fig. 4A) and a 100 mm. increase in precipitation was associated with a 0.8% increase per year in endophyte prevalence (Fig. 4B). This result aligns with the species' autumn active growing season, however other seasonal climate drivers were also associated with increasing endophyte prevalence. In particular, we found cooler and drier springs and cooler summers to be associated with increasing endophyte prevalence (greater than 99% posterior probabilities of negative slopes) however these slopes were generally of smaller magnitude than those for autumn climate drivers.

Changes in endophyte prevalence across the ranges of *A. hyemalis* and *E. virginicus* were less strongly driven by changes in climate. Like *A. perennans*, climate during peak growing season (spring for *A. perennans* and summer for *E. virginicus*) emerged most commonly as drivers of changes in endophyte prevalence. Increases in mean spring precipitation were the strongest predictor of increasing trends in endophyte prevalence for *A. hyemalis* (Fig. 4B) (greater than 99% posterior probability of a positive slope). For this species, an increase of 100 mm. in spring precipitation led to an increase of 0.6% per year in endophyte prevalence. The next greatest slopes were those associated with variability in spring precipitation (greater than 96% posterior probability of a negative slope), as well as in the mean and variability of autumn climate (greater than 98% probability of negative and positive slopes, respectively). Changes in endophyte prevalence in *E. virginicus* were not strongly associated with changes in most climate drivers, but regions with reduced variability in autumn precipitation (Fig. 4B) and with cooler and more variable summer temperatures (Fig. 4A,C) experienced the largest increases in endophyte prevalence. While our analysis identified the importance of these drivers with relatively high certainty (greater than 99% posterior probability of either negative or positive slopes respectively), they translate to less than 0.2% change in endophyte prevalence per year for a change of 100 mm. change in precipitation over the century. Repeating this analysis using all pixels across each species' distribution were qualitatively similar to these results.

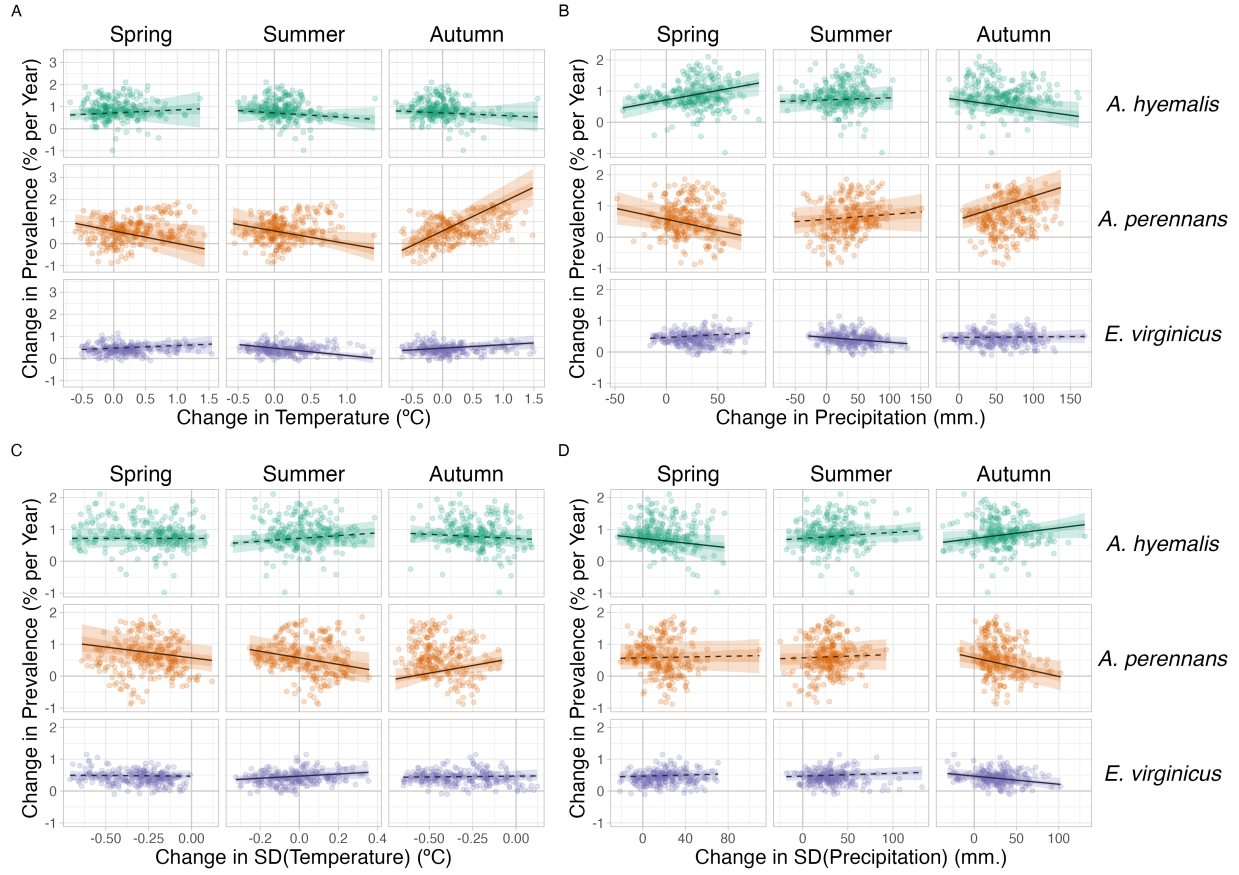


**Figure 4: Relationships between predicted trends in endophyte prevalence and changes in seasonal climate drivers.** Lines show marginal predicted relationship between spatially-varying trends in endophyte prevalence and changes in mean and variability of climate ((A): mean temperature, (B): cumulative precipitation, (C): standard deviation in temperature, (D): standard deviation in precipitation). Confidence bands represent the 50 and 95% CI, colored by host species. Slopes with greater than 95% probability of being either positive or negative are represented as solid lines while those that have less than 95% probability are dashed. Points show 250 randomly sampled pixels across each host's distribution used in model fitting.

387 *Performance on test data*

388 Tests of model's predictive performance as quantified by AUC and by visual posterior predic-  
389 tive checks, indicated good predictive ability. Model performance was similar between historic  
390 herbarium specimens used as training data and the out-of-sample test data from contemporary  
391 surveys (AUC = 0.79 and 0.77 respectively; Fig. A5-A4). The model successfully captured broad  
392 regional trends in endophyte prevalence seen in the contemporary survey data, such as decline  
393 endophyte prevalence in *A. hyemalis* towards western longitudes (Fig. 5A) and northern lati-  
394 tudes (Fig. 5B). However, model predictions for endophyte prevalence exhibited relatively little  
395 local geographic variation, whereas the out-of-sample survey data were maximally variable with  
396 populations spanning 0% to 100% endophyte-symbiotic plants (Fig. 5C). We interpret this to  
397 mean that the model captures coarse-scale spatial and temporal trends reasonably well, but is  
398 not equipped to capture local-scale nuances that generate population-to-population differences.

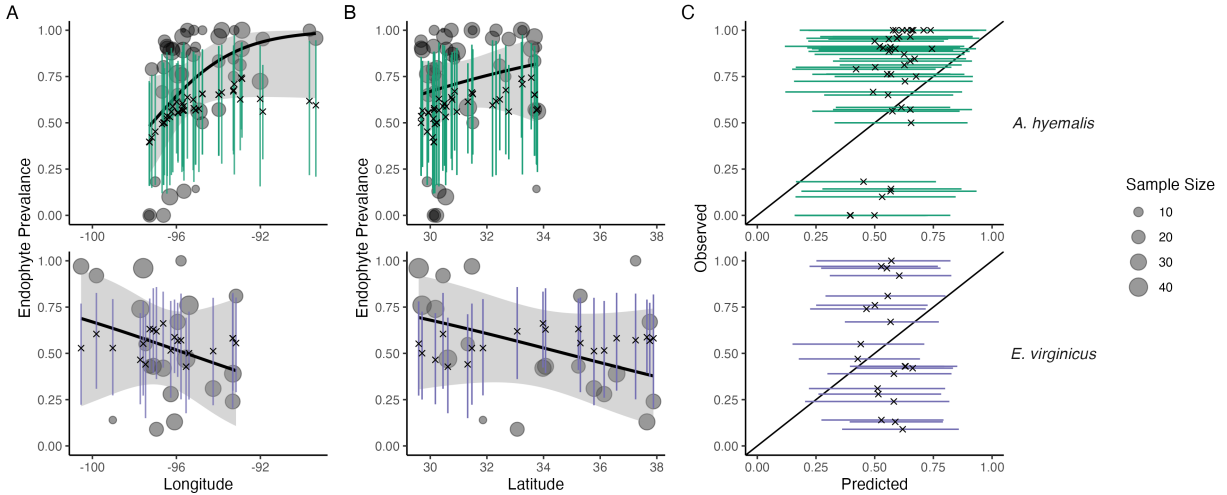


**Figure 5: Predictive performance for contemporary test data.** (A) The model, trained on historic herbarium collection data, performed modestly at predicting prevalence in contemporary population surveys. The model captured regional trends across (A) longitude and (B) latitude. Crosses indicate predicted mean prevalence along with the 95% CI (colored lines) from the herbarium model. Contemporary prevalence is represented by grey points (point size reflects sample size) along with trend lines from generalized linear models (black line and shaded 95% confidence interval). (C) Comparison of observed vs. predicted endophyte prevalence shows that contemporary test data had more variance between populations than contemporary predictions.

## Discussion

Our examination of historic plant specimens revealed cryptic shifts in microbial symbiosis over the last two centuries. For the three host species we examined, there have been strong increases in prevalence of fungal endophytes. We interpret increases in prevalence of *Epichloë*, which are vertically transmitted, as adaptive changes that improve the fitness of their hosts under increasing environmental stress. This interpretation is in line with theory predicting that the positive fitness feedback caused by vertical transmission leads beneficial symbionts to rise in prevalence within a population (Donald et al., 2021; Fine, 1975). We further found that trends in endophyte

407 prevalence varied across the distribution of each species in association with changes in climate  
408 drivers, suggesting that the increases in endophyte prevalence are driven by context-dependent  
409 benefits to hosts that confer resilience under environmental change. Taken together, this suggests  
410 an overall strengthening of host-symbiont mutualism over the last two centuries.

411 Differences across host species underscore that while all of these  $C_3$  grasses share similar  
412 broad-scale distributions, each engages in unique biotic interactions and has unique responses to  
413 environmental drivers. We identified hotspots of change for *A. perennans*, which was the species  
414 that experienced the strongest absolute changes in endophyte prevalence (Fig. 3). Declines of  
415 0.9% per year in the southern portion of its range and increases of up to 2% per year in the  
416 north suggest a potential poleward range shift of endophyte-symbiotic plants (whether the over-  
417 all host distribution is shifting in parallel is an exciting next question). Based on previous work  
418 demonstrating that endophytes can shield their hosts from drought stress (reviewed in Decunta  
419 et al. (2021)), we generally predicted that drought conditions would be a driver of increasing en-  
420 dophyte prevalence. In contrast to this expectation, increasing prevalence for *A. perennans* were  
421 associated with increasing autumn temperature and precipitation (Fig. 4). To our knowledge,  
422 the response of the symbiosis in *A. perennans* to drought has not been examined experimentally,  
423 but in a greenhouse experiment, endophytes had a positive effect on host reproduction under  
424 shaded, low-light conditions (Davitt et al., 2010). Our results also hint that it may be useful to  
425 investigate whether lagged climate effects are important predictors of host fitness in this system  
426 (Evers et al., 2021). Endophyte prevalence of the autumn-flowering *A. perennans* was strongly  
427 linked with decreasing spring precipitation, and that of the spring-flowering *A. hyemalis* was as-  
428 sociated with decreasing autumn precipitation (Fig. 4B). For *A. hyemalis*, endophytes could be  
429 playing a role helping hosts weather autumn-season droughts, which may be an important time  
430 for the species' germination. Previous work has demonstrated drought benefits in a greenhouse  
431 manipulation with this species (Davitt et al., 2011), and early life stages may be particularly vul-  
432 nerable to prolonged droughts. For *E. virginicus*, which experienced the most modest changes  
433 in endophtye prevalence overall (ranging between 1.1% increases and 0.2% decreases), we only

434 found modest associations with changes in climate drivers. Surveys by Sneck et al. (2017), used  
435 as part of the test data in this study, identified a drought index (SPEI) that integrates precipitation  
436 with estimated evapotranspiration as an important predictor of endophyte prevalence. *Epichloë*  
437 endophytes have also been connected to a suite of non-drought related fitness benefits including  
438 herbivore protection (Brem and Leuchtmann, 2001), salinity resistance (Wang et al., 2020), and  
439 mediation of the soil microbiome (Roberts and Ferraro, 2015). These effects are potentially medi-  
440 ated by the diverse bioactive alkaloids and other signaling compounds they produce (Saikkonen  
441 et al., 2013). Increases in symbionts could be explained, at least in part, by these diverse benefits  
442 that may help hosts weather a world made increasingly stressful by changes in climate and other  
443 anthropogenically introduced stressors. While we show consistent increasing trends in preva-  
444 lence between the three species, the mechanisms that explain these changes may be diverse and  
445 idiosyncratic.

446 The combination of a spatially-explicit model and historic herbarium specimens allowed us  
447 to identify regions of both increasing and decreasing endophyte prevalence, however we see  
448 several next steps towards the goal of predicting host and symbiont niche-shifts in response to  
449 future climate change. While the model recreated the large-scale spatial trends observed in con-  
450 temporary population surveys, test data contained more population-to-population variability in  
451 prevalence. Validating our model predictions in this way, a rare extra step in collections-based  
452 studies, allows us to evaluate places to improve the model's out-of-sample predictive ability.  
453 Lack of information on local variability may simply be a feature of data derived from herbarium  
454 specimens. They are samples from local populations, but they are single specimens that are ag-  
455 gregated to derive broad-scale model estimates. This suggests that increasing local replication  
456 should be a factor considered in future collection efforts of natural history specimens, balanced  
457 with the required time and effort. Poor predictive ability at local scales in this grass-endophyte  
458 system is not surprising, as previous studies have found that local variation, even to the scale  
459 of hundreds of meters can structure endophyte-host niches (Kazenel et al., 2015). Other studies  
460 have found factors including land-use history (Vikuk et al., 2019) and the biotic environment,

461 including herbivory (Rudgers et al., 2016), and host genotype Sneck et al. (2017), to be important  
462 predictors of endophyte ecology. An important step would be integrating data from local and  
463 regional scales through modeling to constrain estimates of local and regional variation. Previ-  
464 ous population surveys have found environment-dependent gradients in endophyte prevalence  
465 (Rudgers and Swafford, 2009; Semmarin et al., 2015; Sneck et al., 2017), that may be caused  
466 by symbiont-derived fitness benefits allowing their hosts to persist in environments where they  
467 otherwise could not (Afkhami et al., 2014; Fowler et al., 2023; Kazenel et al., 2015). Predict-  
468 ing future niche-shifts of hosts and symbionts will require considering the coupled dynamics of  
469 host-symbiont dispersal in addition to fitness benefits. For example, transplanting symbiotic and  
470 non-symbiotic plants beyond the range edge of *A. hyemalis* could tell us whether low endophyte  
471 prevalence in that area is a result of environmental conditions that lead the symbiosis to negative  
472 fitness consequences, or is a result of some historical contingency or dispersal limitation that  
473 has thus far limited the presence of symbiotic hosts from a region where they would otherwise  
474 flourish and provide resilience. Incorporating available climatic and soil layers as covariates is  
475 another obvious step that could improve predictions. These steps will bridge gaps that often  
476 exist between large but broad bioclimatic and biodiversity data and small but local data on bi-  
477 otic interactions, and move towards the goal of predicting the dynamics of microbial symbioses  
478 under climate change (Isaac et al., 2020; Miller et al., 2019).

479 Our analysis advances the use of herbarium specimens in global change biology in two ways.  
480 First and foremost, this is the first study to link long-term changes in microbial symbioses to  
481 changes in climate using specimens from natural history collections. The responses of micro-  
482 bial symbioses are a rich target for future studies within museum specimens, particularly those  
483 that take advantage of advances in sequencing technology. While we used relatively coarse  
484 presence/absence data based on fungal morphology, other studies have examined historic plant  
485 microbiomes using molecular sequencing and sophisticated bioinformatics techniques, but these  
486 studies have so far been limited to relatively few specimens at limited spatial extents (Bieker  
487 et al., 2020; Bradshaw et al., 2021; Gross et al., 2021; Heberling and Burke, 2019; Yoshida et al.,

488 2015). Continued advances in capturing historic DNA and in filtering out potential contamina-  
489 tion during specimen storage (Bakker et al., 2020; Daru et al., 2019; Raxworthy and Smith, 2021)  
490 will be imperative in the effort to scale up these efforts. This scaling up will be essential to be  
491 able to quantify changes not just in the prevalence of symbionts, but also in symbionts' intraspe-  
492 cific variation and evolutionary responses to climate change, as well as in changes in the wider  
493 microbial community. Genetic variation in *Epichloë* endophytes, particularly in genes respon-  
494 sible for alkaloid production, produces "chemotypes" with differing benefits for hosts against  
495 insect or mammalian herbivores mediated by environmental conditions (Saikkonen et al., 2013;  
496 Schardl et al., 2012). With improved molecular insights from historic specimens, we could ask  
497 whether the broad increases in endophytes that we have identified reflect selection for particular  
498 chemotypes and how this selection varies across space. Answering these questions as well as  
499 the unknown questions that future researchers may ask also reiterates the value in capturing  
500 meta-information during ongoing digitization efforts at herbaria around the world and during  
501 the accession of newly collected specimens (Edwards et al.; Lendemer et al., 2020). Second, we  
502 accounted for several potential biases in the data observation process that may be common to  
503 many collections-based research questions by using a spatially-explicit random effects model.  
504 Spatial autocorrelation (Willems et al., 2022), potential biases introduced by the sampling habits  
505 of collectors (Daru et al., 2018), and variation between contemporary researchers during the col-  
506 lection of trait data, if not corrected for could lead to over-confident inference about the strength  
507 and direction of historic change (Fig. 2). Previous studies that have quantified the effects of  
508 collector biases typically find them to be small (Davis et al., 2015; Meineke et al., 2019), and we  
509 similarly did not find that collector has a strong effect on the results of our analysis, but that  
510 scorer identity did impact results.

511        Ultimately, a central goal of global change biology is to generate predictive insights into the  
512 future of natural systems on a rapidly changing planet. Beyond host-microbe symbioses, de-  
513 tecting ecological responses to anthropogenic global change and attributing their causes would  
514 inform public policy decision-makers and adaptive management strategies. This survey of his-

515 toric endophyte prevalence is necessarily correlative, yet it serves as a foundation to develop  
516 better predictive models of the response of microbial symbioses to climate change. By compar-  
517 ing detected ecological responses with alternative mechanistic simulations of the past, we could  
518 attribute their cause, in a manner similar to methods from climate science and economics (Car-  
519 leton and Hsiang, 2016; Stott et al., 2010; Trenberth et al., 2015). Combining the insights from  
520 this type of regional-scale survey with field experiments and physiological performance data  
521 could be invaluable to identify mechanisms driving shifts in host-symbiont dynamics. Evidence  
522 is strong that certain dimensions of climate change correlated with endophytes' temporal re-  
523 sponses, however we do not know why trends in prevalence were weak in some areas or how  
524 endophytes would respond to more extreme changes in climate. The "time machine" of natu-  
525 ral history collections revealed evidence of mutualism resilience for grass-endophyte symbioses  
526 in the face of environmental change, but more extreme changes could potentially push one or  
527 both partners beyond their physiological limits, leading to the collapse of the mutualism; more  
528 research is needed to understand what those limits might be.

529 **Acknowledgments**

530 We thank Dr. Jessica Budke for help in drafting our initial destructive sampling plan, and to the  
531 many staff members of herbaria who facilitated our research visits, as well as to the hundreds  
532 of collectors who contributed to the natural history collections. Several high schooler and un-  
533 dergraduate researchers contributed to data collection, including A. Appio-Riley, P. Bilderback,  
534 E. Chong, K. Dickens, L. Dufresne, B. Gutierrez, A. Johnson, S. Linder, E. Scales, B. Scherick,  
535 K. Schrader, E. Segal , G. Singla, and M. Tucker. This research was supported by funding from  
536 National Science Foundation (grants 1754468 and 2208857) and by funding from the Texas Ecolab  
537 Program.

538

## Statement of Authorship

539 J.C.F. contributed to research conception, data collection, data analysis, and led manuscript draft-  
540 ing. J.M. contributed to data analysis and manuscript revisions. T.E.X.M. contributed to research  
541 conception, data collection, data analysis, and manuscript revisions.

542

## Data and Code Availability

543 Data from this publication can be found through a publicly available repository  
544 (<https://doi.org/10.5061/dryad.rn8pk0pn0>). Code for analyses can be found through a pub-  
545 licly available repository (<https://github.com/joshuacfowler/EndoHerbarium>) that will be per-  
546 manently archived upon publication.

## Literature Cited

- 548 M E Afkhami. Fungal endophyte–grass symbioses are rare in the California floristic province and  
549 other regions with mediterranean-influenced climates. *Fungal Ecology*, 5(3):345–352, 2012.
- 550 M E Afkhami and J A Rudgers. Symbiosis lost: Imperfect vertical transmission of fungal endo-  
551 phytes in grasses. *The American Naturalist*, 172(3):405–416, 2008.
- 552 M E Afkhami, P J McIntyre, and S Y Strauss. Mutualist-mediated effects on species' range limits  
553 across large geographic scales. *Ecology Letters*, 17(10):1265–1273, 2014.
- 554 S N Aitken, S Yeaman, J A Holliday, T Wang, and S Curtis-McLane. Adaptation, migration  
555 or extirpation: Climate change outcomes for tree populations. *Evolutionary Applications*, 1(1):  
556 95–111, 2008.
- 557 C E Aslan, E S Zavaleta, B Tershy, and D Croll. Mutualism disruption threatens global plant  
558 biodiversity: a systematic review. *PloS one*, 8(6):e66993, 2013.
- 559 F E Bachl, F Lindgren, D L Borchers, and J B Illian. inlabru: an R package for Bayesian spatial  
560 modelling from ecological survey data. *Methods in Ecology and Evolution*, 10(6):760–766, 2019.
- 561 C W Bacon and J F White. Stains, media, and procedures for analyzing endophytes. In *Biotech-  
562 nology of endophytic fungi of grasses*, pages 47–56. CRC Press, 2018.
- 563 H Bakka, H Rue, G-A Fuglstad, A Riebler, D Bolin, J Illian, E Krainski, D Simpson, and F Lind-  
564 gren. Spatial modeling with r-inla: A review. *Wiley Interdisciplinary Reviews: Computational  
565 Statistics*, 10(6):e1443, 2018.
- 566 F T Bakker, V C Bieker, and M D Martin. Herbarium collection-based plant evolutionary genetics  
567 and genomics. *Frontiers in Ecology and Evolution*, 8:603948, 2020.
- 568 D R Bazely, J P Ball, M Vicari, A J Tanentzap, M Bérenger, T Rakocevic, and S Koh. Broad-scale

- 569 geographic patterns in the distribution of vertically-transmitted, asexual endophytes in four  
570 naturally-occurring grasses in sweden. *Ecography*, 30(3):367–374, 2007.
- 571 J Beguin, S Martino, H Rue, and S G Cumming. Hierarchical analysis of spatially autocorrelated  
572 ecological data using integrated nested laplace approximation. *Methods in Ecology and Evolution*,  
573 3(5):921–929, 2012.
- 574 C S Berg, J L Brown, and J J Weber. An examination of climate-driven flowering-time shifts at  
575 large spatial scales over 153 years in a common weedy annual. *American Journal of Botany*, 106  
576 (11):1435–1443, 2019.
- 577 V C Bieker, F Sánchez Barreiro, J A Rasmussen, M Brunier, N Wales, and M D Martin. Metage-  
578 nomic analysis of historical herbarium specimens reveals a postmortem microbial community.  
579 *Molecular Ecology Resources*, 20(5):1206–1219, 2020.
- 580 J L Blois, P L Zarnetske, M C Fitzpatrick, and S Finnegan. Climate change and the past, present,  
581 and future of biotic interactions. *Science*, 341(6145):499–504, 2013.
- 582 M Bradshaw, U Braun, M Elliott, J Kruse, S-Y Liu, G Guan, and P Tobin. A global genetic analysis  
583 of herbarium specimens reveals the invasion dynamics of an introduced plant pathogen. *Fungal*  
584 *Biology*, 125(8):585–595, 2021.
- 585 D Brem and A Leuchtmann. *Epichloë* grass endophytes increase herbivore resistance in the wood-  
586 land grass *Brachypodium sylvaticum*. *Oecologia*, 126(4):522–530, 2001.
- 587 T A Carleton and S M Hsiang. Social and economic impacts of climate. *Science*, 353(6304):  
588 aad9837, 2016.
- 589 S Cheng, Y-N Zou, K Kuča, A Hashem, E F Abd\_Allah, and Q-S Wu. Elucidating the mechanisms  
590 underlying enhanced drought tolerance in plants mediated by arbuscular mycorrhizal fungi.  
591 *Frontiers in Microbiology*, 12:4029, 2021.

- 592 K Clay and C Schardl. Evolutionary origins and ecological consequences of endophyte symbiosis  
593 with grasses. *The American Naturalist*, 160(S4):S99–S127, 2002.
- 594 D G Clayton, L Bernardinelli, and C Montomoli. Spatial correlation in ecological analysis. *Inter-*  
595 *national Journal of Epidemiology*, 22(6):1193–1202, 1993.
- 596 KD Craven, PTW Hsiao, A Leuchtmann, W Hollin, and CL Schardl. Multigene phylogeny of  
597 *Epichloë* species, fungal symbionts of grasses. *Annals of the Missouri Botanical Garden*, pages  
598 14–34, 2001.
- 599 K M Crawford, J M Land, and J A Rudgers. Fungal endophytes of native grasses decrease insect  
600 herbivore preference and performance. *Oecologia*, 164:431–444, 2010.
- 601 M S Crossley, T D Meehan, M D Moran, J Glassberg, W E Snyder, and A K Davis. Opposing  
602 global change drivers counterbalance trends in breeding North American monarch butterflies.  
603 *Global Change Biology*, 28(15):4726–4735, 2022.
- 604 C Daly and K Bryant. The PRISM climate and weather system — An introduction. *Corvallis, OR:*  
605 *PRISM climate group*, 2, 2013.
- 606 B H Daru, D S Park, R B Primack, C G Willis, D S Barrington, T J S Whitfeld, T G Seidler, P W  
607 Sweeney, D R Foster, A M Ellison, et al. Widespread sampling biases in herbaria revealed from  
608 large-scale digitization. *New Phytologist*, 217(2):939–955, 2018.
- 609 B H Daru, E A Bowman, D H Pfister, and A E Arnold. A novel proof of concept for capturing  
610 the diversity of endophytic fungi preserved in herbarium specimens. *Philosophical Transactions*  
611 *of the Royal Society B*, 374(1763):20170395, 2019.
- 612 C C Davis, C G Willis, B Connolly, C Kelly, and A M Ellison. Herbarium records are reliable  
613 sources of phenological change driven by climate and provide novel insights into species'  
614 phenological cueing mechanisms. *American Journal of Botany*, 102(10):1599–1609, 2015.

- 615 A J Davitt, M Stansberry, and H A Rudgers. Do the costs and benefits of fungal endophyte  
616 symbiosis vary with light availability? *New Phytologist*, 188(3):824–834, 2010.
- 617 A J Davitt, C Chen, and J A Rudgers. Understanding context-dependency in plant–microbe  
618 symbiosis: The influence of abiotic and biotic contexts on host fitness and the rate of symbiont  
619 transmission. *Environmental and Experimental Botany*, 71(2):137–145, 2011.
- 620 F A Decunta, L I Pérez, D P Malinowski, M A Molina-Montenegro, and P E Gundel. A systematic  
621 review on the effects of *Epichloë* fungal endophytes on drought tolerance in cool-season grasses.  
622 *Frontiers in Plant Science*, 12:644731, 2021.
- 623 M Di Luzio, G L Johnson, C Daly, J K Eischeid, and J G Arnold. Constructing retrospective grid-  
624 ded daily precipitation and temperature datasets for the conterminous United States. *Journal*  
625 *of Applied Meteorology and Climatology*, 47(2):475–497, 2008.
- 626 M L Donald, T F Bohner, K M Kolis, R A Shadow, J A Rudgers, and T E Miller. Context-  
627 dependent variability in the population prevalence and individual fitness effects of plant–  
628 fungal symbiosis. *Journal of Ecology*, 109(2):847–859, 2021.
- 629 AE Douglas. Host benefit and the evolution of specialization in symbiosis. *Heredity*, 81(6):599–  
630 603, 1998.
- 631 Y-W Duan, H Ren, T Li, L-L Wang, Z-Q Zhang, Y-L Tu, and Y-P Yang. A century of pollination  
632 success revealed by herbarium specimens of seed pods. *New Phytologist*, 224(4):1512–1517,  
633 2019.
- 634 E J Edwards, B D Mishler, and C D Davis. University herbaria are uniquely important. *Trends in*  
635 *Plant Science*.
- 636 M Engel, T Mette, and W Falk. Spatial species distribution models: Using Bayes inference with  
637 INLA and SPDE to improve the tree species choice for important European tree species. *Forest*  
638 *Ecology and Management*, 507:119983, 2022.

- 639 S M Evers, T M Knight, D W Inouye, TEX Miller, R Salguero-Gómez, A M Iler, and A Com-  
640 pagnoni. Lagged and dormant season climate better predict plant vital rates than climate  
641 during the growing season. *Global Change Biology*, 27(9):1927–1941, 2021.
- 642 P E M Fine. Vectors and vertical transmission: an epidemiologic perspective. *Annals of the New  
643 York Academy of Sciences*, 266(1):173–194, 1975.
- 644 J C Fowler, M L Donald, J L Bronstein, and TEX Miller. The geographic footprint of mutualism:  
645 How mutualists influence species' range limits. *Ecological Monographs*, 93(1):e1558, 2023.
- 646 J C Fowler, S Ziegler, K D Whitney, J A Rudgers, and TEX Miller. Microbial symbionts buffer  
647 hosts from the demographic costs of environmental stochasticity. *Ecology Letters*, 27(5):e14438,  
648 2024.
- 649 PR Frade, F De Jongh, F Vermeulen, J Van Bleijswijk, and RPM Bak. Variation in symbiont  
650 distribution between closely related coral species over large depth ranges. *Molecular Ecology*,  
651 17(2):691–703, 2008.
- 652 M E Frederickson. Mutualisms are not on the verge of breakdown. *Trends in Ecology & Evolution*,  
653 32(10):727–734, 2017.
- 654 S E Gilman, M C Urban, J Tewksbury, G W Gilchrist, and R D Holt. A framework for community  
655 interactions under climate change. *Trends in Ecology & Evolution*, 25(6):325–331, 2010.
- 656 G Granath, M Vicari, D R Bazely, J P Ball, A Puentes, and T Rakocevic. Variation in the abundance  
657 of fungal endophytes in fescue grasses along altitudinal and grazing gradients. *Ecography*, 30  
658 (3):422–430, 2007.
- 659 A Gross, C Petitcollin, C Dutech, B Ly, M Massot, J Faivre d'Arcier, L Dubois, G Saint-Jean, and  
660 M-L Desprez-Loustau. Hidden invasion and niche contraction revealed by herbaria specimens  
661 in the fungal complex causing oak powdery mildew in europe. *Biological Invasions*, 23:885–901,  
662 2021.

- 663 E K Hart and K Bell. *prism: Download data from the Oregon prism project*, 2015. URL  
664 <https://github.com/ropensci/prism>. R package version 0.0.6.
- 665 J J Heberling and D J Burke. Utilizing herbarium specimens to quantify historical mycorrhizal  
666 communities. *Applications in plant sciences*, 7(4):e01223, 2019.
- 667 R J Hijmans, S Phillips, J Leathwick, J Elith, and Robert J Hijmans. Package ‘dismo’. *Circles*, 9(1):  
668 1–68, 2017.
- 669 J HilleRisLambers, M A Harsch, A K Ettinger, K R Ford, and E J Theobald. How will biotic  
670 interactions influence climate change-induced range shifts? *Annals of the New York Academy of  
671 Sciences*, 1297(1):112–125, 2013.
- 672 IPCC. Climate change 2021: The physical science basis, 2021. URL  
673 <https://www.ipcc.ch/report/ar6/wg1/>.
- 674 N J B Isaac, M A Jarzyna, P Keil, L I Dambly, P H Boersch-Supan, E Browning, S N Freeman,  
675 N Golding, G Guillera-Arroita, P A Henrys, et al. Data integration for large-scale models of  
676 species distributions. *Trends in Ecology & Evolution*, 35(1):56–67, 2020.
- 677 A Jiménez-Valverde. Insights into the area under the receiver operating characteristic curve (auc)  
678 as a discrimination measure in species distribution modelling. *Global Ecology and Biogeography*,  
679 21(4):498–507, 2012.
- 680 D Kahle and H Wickham. Package ‘ggmap’. *Retrieved September*, 5:2021, 2019.
- 681 M R Kazenel, C L Debban, L Ranelli, W Q Hendricks, Y A Chung, T H Pendergast IV, N D  
682 Charlton, C A Young, and J A Rudgers. A mutualistic endophyte alters the niche dimensions  
683 of its host plant. *AoB plants*, 7:plv005, 2015.
- 684 R A Knapp, G M Fellers, P M Kleeman, D AW Miller, V T Vredenburg, E B Rosenblum, and  
685 C J Briggs. Large-scale recovery of an endangered amphibian despite ongoing exposure to  
686 multiple stressors. *Proceedings of the National Academy of Sciences*, 113(42):11889–11894, 2016.

- 687 M V Kozlov, I V Sokolova, V Zverev, A A Egorov, M Y Goncharov, and E L Zvereva. Biases in  
688 estimation of insect herbivory from herbarium specimens. *Scientific Reports*, 10(1):12298, 2020.
- 689 B R Lee, E F Alecrim, T K Miller, J RK Forrest, J M Heberling, R B Primack, and R D Sargent.  
690 Phenological mismatch between trees and wildflowers: Reconciling divergent findings in two  
691 recent analyses. *Journal of Ecology*, 112(6):1184–1199, 2024.
- 692 J Lendemer, B Thiers, A K Monfils, J Zaspel, E R Ellwood, A Bentley, K LeVan, J Bates, D Jennings,  
693 D Contreras, et al. The extended specimen network: A strategy to enhance us biodiversity  
694 collections, promote research and education. *BioScience*, 70(1):23–30, 2020.
- 695 A Leuchtmann. Systematics, distribution, and host specificity of grass endophytes. *Natural Toxins*,  
696 1(3):150–162, 1992.
- 697 A Leuchtmann, C W Bacon, C L Schardl, J F White Jr, and M Tadych. Nomenclatural realignment  
698 of *Neotyphodium* species with genus *Epichloë*. *Mycologia*, 106(2):202–215, 2014.
- 699 F Lindgren, H Rue, and J Lindström. An explicit link between gaussian fields and gaussian  
700 markov random fields: the stochastic partial differential equation approach. *Journal of the Royal  
701 Statistical Society: Series B (Statistical Methodology)*, 73(4):423–498, 2011.
- 702 C Liu, P M Berry, T P Dawson, and R G Pearson. Selecting thresholds of occurrence in the  
703 prediction of species distributions. *Ecography*, 28(3):385–393, 2005.
- 704 M McFall-Ngai, M G Hadfield, TCG Bosch, H V Carey, T Domazet-Lošo, A E Douglas, N Dubilier,  
705 G Eberl, T Fukami, S F Gilbert, et al. Animals in a bacterial world, a new imperative for the  
706 life sciences. *Proceedings of the National Academy of Sciences*, 110(9):3229–3236, 2013.
- 707 T D Meehan, N L Michel, and H Rue. Spatial modeling of Audubon Christmas Bird Counts  
708 reveals fine-scale patterns and drivers of relative abundance trends. *Ecosphere*, 10(4):e02707,  
709 2019.

- 710 E K Meineke, C C Davis, and T J Davies. The unrealized potential of herbaria for global change  
711 biology. *Ecological Monographs*, 88(4):505–525, 2018.
- 712 E K Meineke, A T Classen, N J Sanders, and T J Davies. Herbarium specimens reveal increasing  
713 herbivory over the past century. *Journal of Ecology*, 107(1):105–117, 2019.
- 714 A R Meyer, M Valentin, L Liulevicius, T R McDonald, M P Nelsen, J Pengra, R J Smith, and  
715 D Stanton. Climate warming causes photobiont degradation and carbon starvation in a boreal cli-  
716 mate sentinel lichen. *American Journal of Botany*, 2022.
- 717 D AW Miller, K Pacifici, J S Sanderlin, and B J Reich. The recent past and promising future for  
718 data integration methods to estimate species' distributions. *Methods in Ecology and Evolution*,  
719 10(1):22–37, 2019.
- 720 D S Park, I Breckheimer, A C Williams, E Law, A M Ellison, and C C Davis. Herbarium speci-  
721 mens reveal substantial and unexpected variation in phenological sensitivity across the eastern  
722 United States. *Philosophical Transactions of the Royal Society B*, 374(1763):20170394, 2019.
- 723 M Parniske. Arbuscular mycorrhiza: The mother of plant root endosymbioses. *Nature Reviews  
724 Microbiology*, 6(10):763–775, 2008.
- 725 A Pauw and J A Hawkins. Reconstruction of historical pollination rates reveals linked declines  
726 of pollinators and plants. *Oikos*, 120(3):344–349, 2011.
- 727 S Piao, Q Liu, A Chen, I A Janssens, Y Fu, J Dai, L Liu, X Lian, M Shen, and X Zhu. Plant phe-  
728 nology and global climate change: Current progresses and challenges. *Global Change Biology*,  
729 25(6):1922–1940, 2019.
- 730 T Poisot, G Bergeron, K Cazelles, T Dallas, D Gravel, A MacDonald, B Mercier, C Violet, and  
731 S Vissault. Global knowledge gaps in species interaction networks data. *Journal of Biogeography*,  
732 48(7):1552–1563, 2021.

- 733 N E Rafferty, P J CaraDonna, and J L Bronstein. Phenological shifts and the fate of mutualisms.
- 734 *Oikos*, 124(1):14–21, 2015.
- 735 C J Raxworthy and B T Smith. Mining museums for historical DNA: Advances and challenges
- 736 in museomics. *Trends in Ecology & Evolution*, 36(11):1049–1060, 2021.
- 737 F Renoz, I Pons, and T Hance. Evolutionary responses of mutualistic insect–bacterial symbioses
- 738 in a world of fluctuating temperatures. *Current Opinion in Insect Science*, 35:20–26, 2019.
- 739 E L Roberts and A Ferraro. Rhizosphere microbiome selection by *Epichloë* endophytes of *Festuca*
- 740 *arundinacea*. *Plant and Soil*, 396:229–239, 2015.
- 741 RJ Rodriguez, JF White Jr, Anne E Arnold, and a RS and Redman. Fungal endophytes: diversity
- 742 and functional roles. *New Phytologist*, 182(2):314–330, 2009.
- 743 G Rolshausen, F Dal Grande, A D Sadowska-Deś, J Otte, and I Schmitt. Quantifying the climatic
- 744 niche of symbiont partners in a lichen symbiosis indicates mutualist-mediated niche expan-
- 745 sions. *Ecography*, 41(8):1380–1392, 2018.
- 746 J A Rudgers, M E Afkhami, M A Rúa, A J Davitt, S Hammer, and V M Huguet. A fungus among
- 747 us: broad patterns of endophyte distribution in the grasses. *Ecology*, 90(6):1531–1539, 2009.
- 748 J A Rudgers, R A Fletcher, E Olivas, C A Young, N D Charlton, D E Pearson, and J L Maron. Long-
- 749 term ungulate exclusion reduces fungal symbiont prevalence in native grasslands. *Oecologia*,
- 750 181:1151–1161, 2016.
- 751 Jennifer A Rudgers and Angela L Swafford. Benefits of a fungal endophyte in *Elymus virginicus*
- 752 decline under drought stress. *Basic and Applied Ecology*, 10(1):43–51, 2009.
- 753 H Rue, S Martino, and N Chopin. Approximate bayesian inference for latent gaussian models
- 754 by using integrated nested laplace approximations. *Journal of the royal statistical society: Series b*
- 755 (*statistical methodology*), 71(2):319–392, 2009.

- 756 K Saikkonen, P E Gundel, and M Helander. Chemical ecology mediated by fungal endophytes  
757 in grasses. *Journal of chemical ecology*, 39:962–968, 2013.
- 758 C L Schardl, C A Young, J R Faulkner, S Florea, and J Pan. Chemotypic diversity of *Epichloae*,  
759 fungal symbionts of grasses. *Fungal Ecology*, 5(3):331–344, 2012.
- 760 María Semmartin, Marina Omacini, Pedro E Gundel, and Ignacio M Hernández-Agramonte.  
761 Broad-scale variation of fungal-endophyte incidence in temperate grasses. *Journal of Ecology*,  
762 103(1):184–190, 2015.
- 763 Michelle E Sneck, Jennifer A Rudgers, Carolyn A Young, and Tom EX Miller. Variation in the  
764 prevalence and transmission of heritable symbionts across host populations in heterogeneous  
765 environments. *Microbial Ecology*, 74:640–653, 2017.
- 766 T F Stocker, D Qin, G-K Plattner, L V Alexander, S K Allen, N L Bindoff, F-M Bréon, J A Church,  
767 U Cubasch, S Emori, et al. Technical summary. In *Climate Change 2013: The Physical Science  
768 Basis. Contribution of Working Group I to the Fifth Assessment Report of the Intergovernmental Panel  
769 on Climate Change*, pages 33–115. Cambridge University Press, 2013.
- 770 P A Stott, N P Gillett, G C Hegerl, D J Karoly, D A Stone, X Zhang, and F Zwiers. Detection and  
771 attribution of climate change: A regional perspective. *Wiley Interdisciplinary Reviews: Climate  
772 Change*, 1(2):192–211, 2010.
- 773 S Sully, DE Burkepile, MK Donovan, G Hodgson, and R Van Woesik. A global analysis of coral  
774 bleaching over the past two decades. *Nature communications*, 10(1):1–5, 2019.
- 775 E Toby Kiers, T M Palmer, A R Ives, J F Bruno, and J L Bronstein. Mutualisms in a changing  
776 world: an evolutionary perspective. *Ecology Letters*, 13(12):1459–1474, 2010.
- 777 A T Tredennick, G Hooker, S P Ellner, and P B Adler. A practical guide to selecting models for  
778 exploration, inference, and prediction in ecology. *Ecology*, 102(6):e03336, 2021.

- 779 K E Trenberth, J T Fasullo, and T G Shepherd. Attribution of climate extreme events. *Nature Climate Change*, 5(8):725–730, 2015.
- 781 A M Truitt, M Kapun, R Kaur, and W J Miller. Wolbachia modifies thermal preference in  
782 *drosophila melanogaster*. *Environmental microbiology*, 21(9):3259–3268, 2019.
- 783 Shripad D. Tuljapurkar. Population dynamics in variable environments. III. Evo-  
784 lutionary dynamics of r-selection. *Theoretical Population Biology*, 21(1):141–165,  
785 February 1982. ISSN 0040-5809. doi: 10.1016/0040-5809(82)90010-7. URL  
786 <http://www.sciencedirect.com/science/article/pii/0040580982900107>.
- 787 A Urdangarin, T Goicoa, and M D Ugarte. Evaluating recent methods to overcome spatial con-  
788 founding. *Revista Matemática Complutense*, 36(2):333–360, 2023.
- 789 V Vikuk, C A Young, S T Lee, P Nagabhyru, M Krischke, M J Mueller, and J Krauss. Infection rates  
790 and alkaloid patterns of different grass species with systemic *Epichloë* endophytes. *Applied and  
791 Environmental Microbiology*, 85(17):e00465–19, 2019.
- 792 Z Wang, C Li, and J White. Effects of *Epichloë* endophyte infection on growth, physiological  
793 properties and seed germination of wild barley under saline conditions. *Journal of Agronomy  
794 and Crop Science*, 206(1):43–51, 2020.
- 795 R J Warren and M A Bradford. Mutualism fails when climate response differs between interacting  
796 species. *Global Change Biology*, 20(2):466–474, 2014.
- 797 N S Webster, R E Cobb, and A P Negri. Temperature thresholds for bacterial symbiosis with a  
798 sponge. *The ISME journal*, 2(8):830–842, 2008.
- 799 J F White and G T Cole. Endophyte-host associations in forage grasses. i. Distribution of fungal  
800 endophytes in some species of *Lolium* and *Festuca*. *Mycologia*, 77(2):323–327, 1985.
- 801 F M Willems, JF Scheepens, and O Bossdorf. Forest wildflowers bloom earlier as europe warms:  
802 Lessons from herbaria and spatial modelling. *New Phytologist*, 235(1):52–65, 2022.

- 803 C G Willis, E R Ellwood, R B Primack, C C Davis, K D Pearson, A S Gallinat, J M Yost, G Nelson,
- 804 S J Mazer, N L Rossington, et al. Old plants, new tricks: Phenological research using herbarium
- 805 specimens. *Trends in Ecology & Evolution*, 32(7):531–546, 2017.
- 806 C Xia, N Li, Y Zhang, C Li, X Zhang, and Z Nan. Role of *Epichloë* endophytes in defense responses
- 807 of cool-season grasses to pathogens: A review. *Plant Disease*, 102(11):2061–2073, 2018.
- 808 K Yoshida, E Sasaki, and S Kamoun. Computational analyses of ancient pathogen DNA from
- 809 herbarium samples: Challenges and prospects. *Frontiers in Plant Science*, 6:771, 2015.

## Appendix A

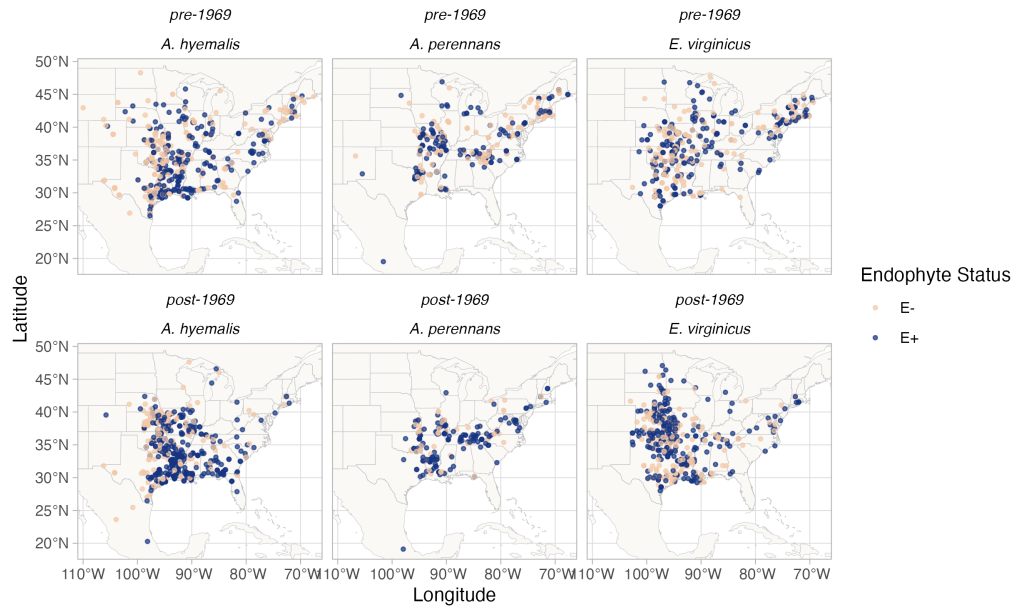


**Figure A1: Endophyte presence/absence in specimens of each host species.** Points show collection locations colored according to whether the specimen contained endophytes ( E+; blue points) or did not contain endophytes (E-, tan points). To visualize temporal change, the data are faceted before and after the median year of collection.

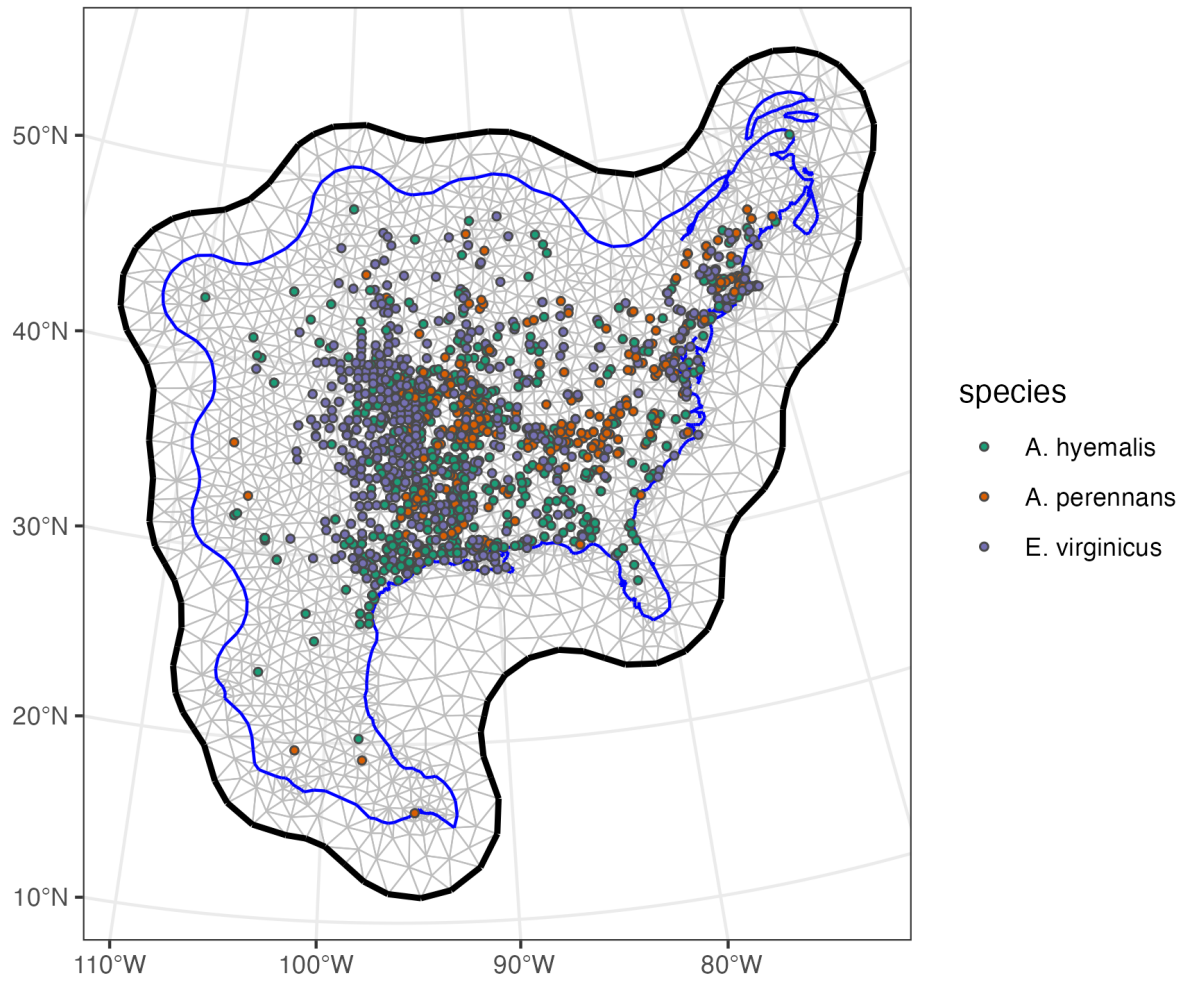


**Figure A2: Triangulation mesh used to estimate spatial dependence between data points.** Grey lines indicate edges of triangles used to define distances between observations. Colored points indicate locations of sampled herbarium specimens for each host species, and the blue line shows the convex hull and coastline used to define the edge of the mesh around the data points. The thick black line shows the convex hull defining a buffer space around the edge of the mesh to reduce the influence of edge effects on model estimates.

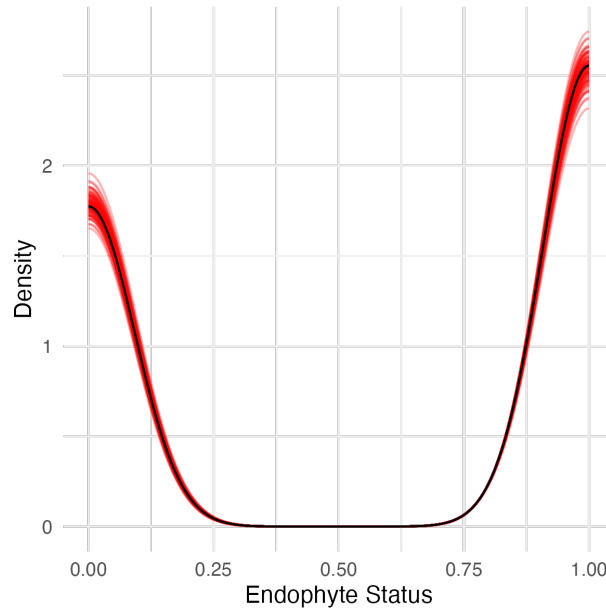


**Figure A3: Consistency between real data and simulated values indicate that the fitted model accurately describes the data.** Graph shows density curves for the observed data (black) along with 100 simulated datasets (red).

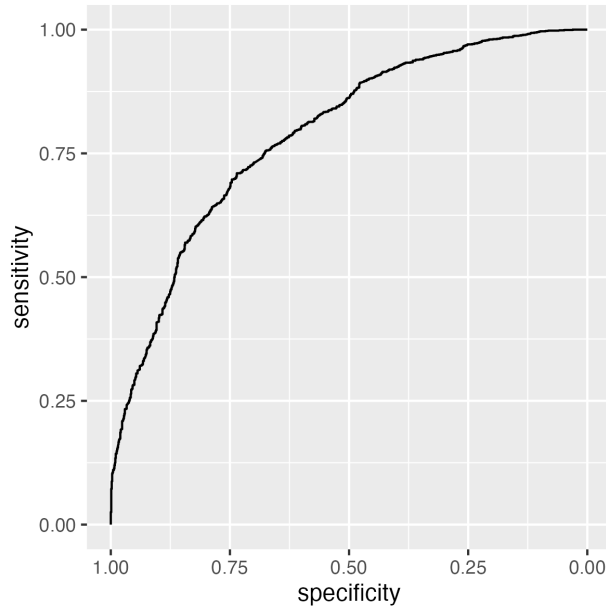


**Figure A4: ROC plot showing model performance classifying observations according to endophyte status within the in-sample data.** The curves show adequate model performance for observed data. The AUC value is 0.79.

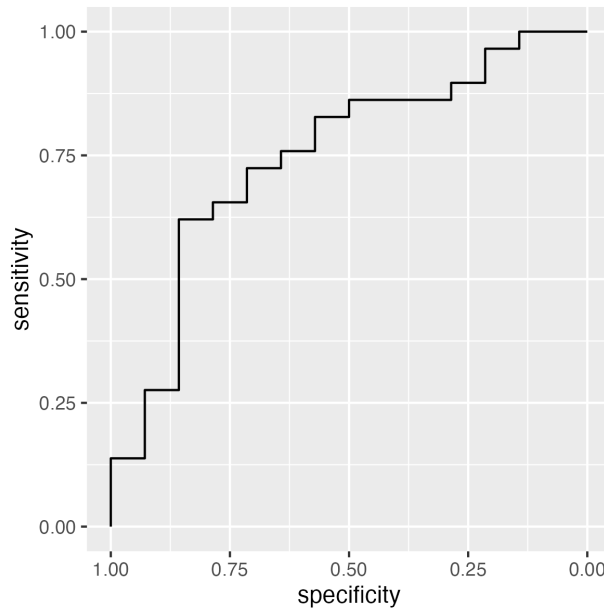


**Figure A5: ROC plot showing model performance classifying observations according to endophyte status within the out-of-sample data.** The curves show adequate model performance for test data. The AUC value is 0.77.

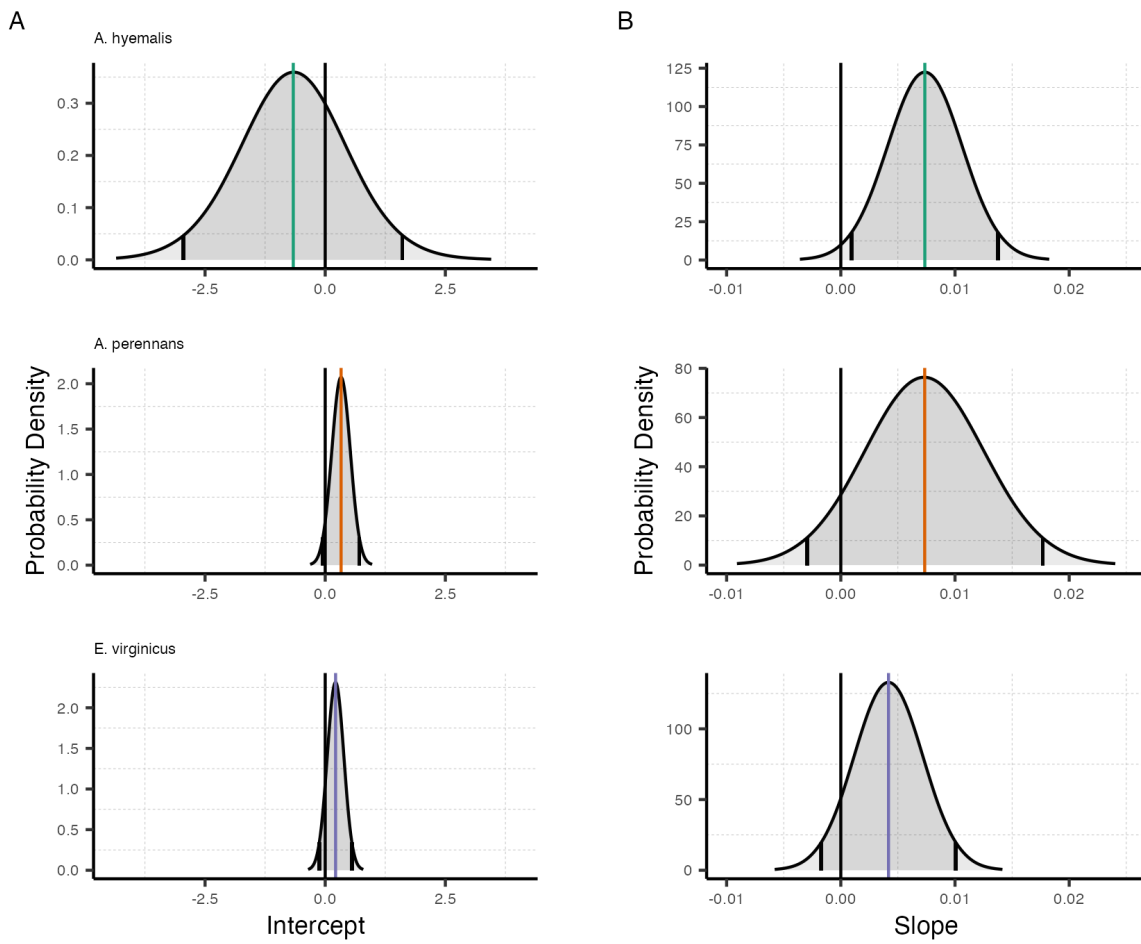


Figure A6: Density curves show the probability density along with mean (colored line) and 95% CI (black lines) for the (A) intercept and (B) slope terms, **A** and **T** respectively. Colors represent each host species

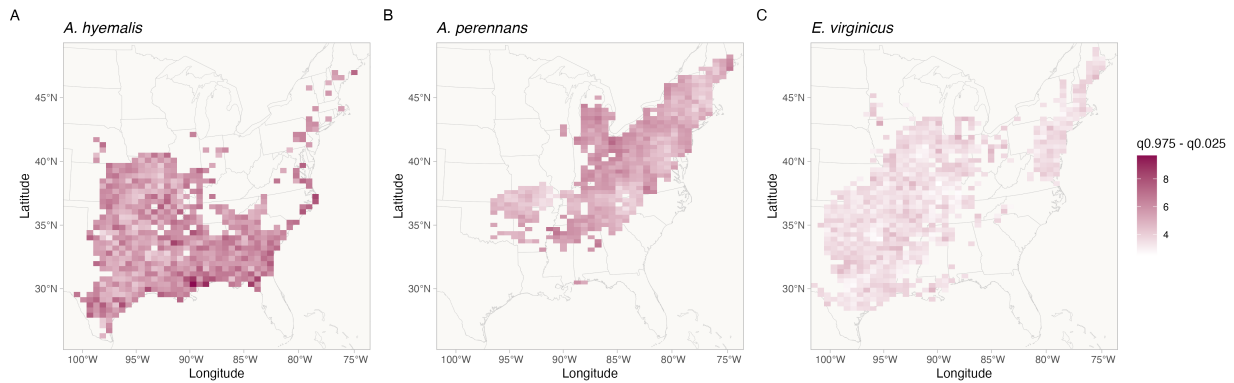


Figure A7: Shading represents the range of the 95% posterior credible interval for spatially varying slopes,  $\tau$ .

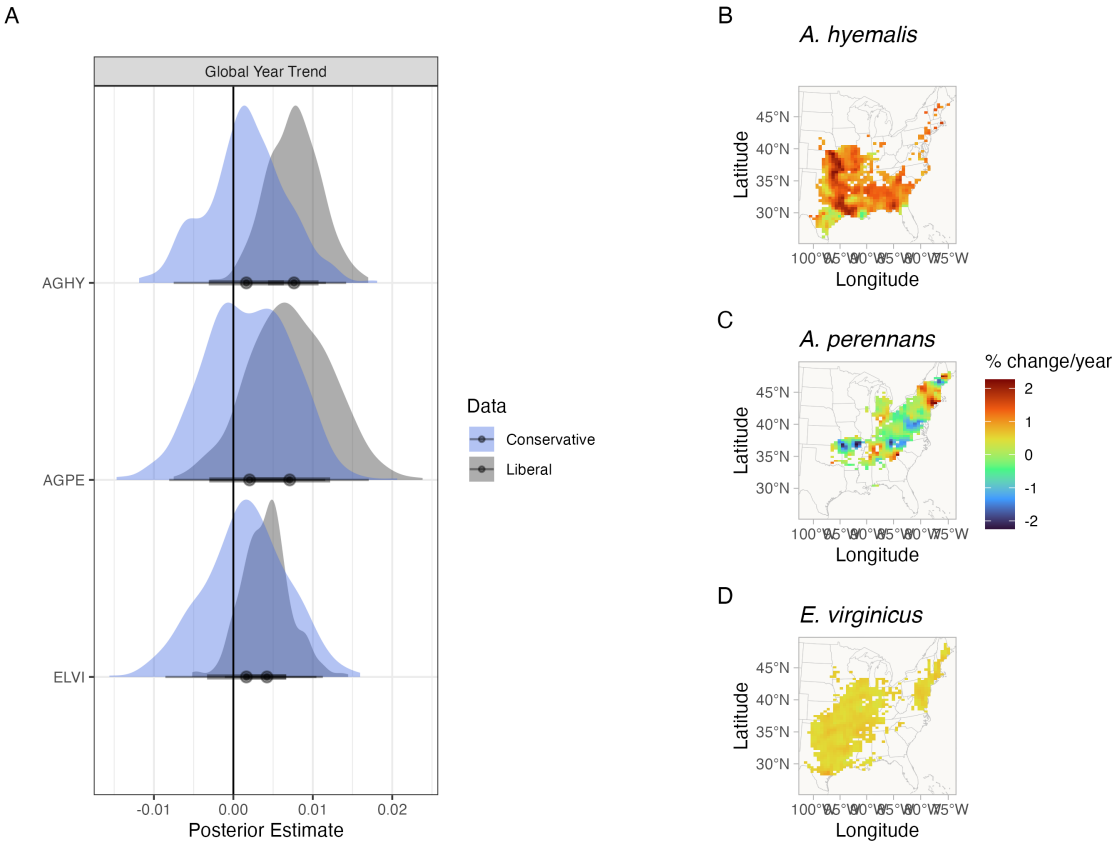


Figure A8: Comparison of liberal versus conservative endophyte scores on modeled outcomes. (A) Posterior estimates of global temporal trend for models fit to liberal scores (grey) and to conservative scores (blue). Maps show the spatially varying temporal trend estimates from model fit to conservative scores for (B) *A. hyemalis*, (C) *A. perennans*, and (D) *E. virginicus*. Note that the color scale differs between this visualization and Fig. 3.

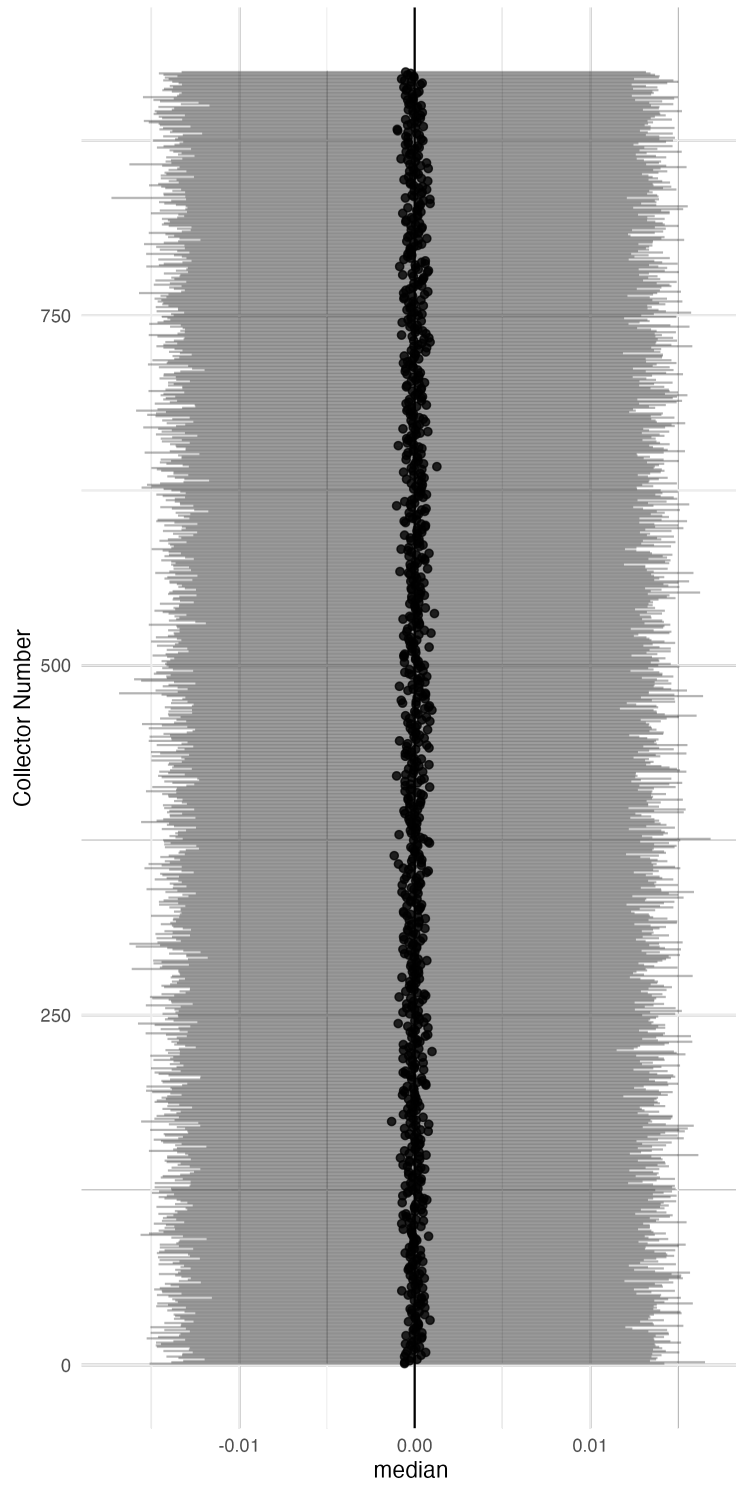


Figure A9: **Posterior estimates of collector random effects.** Points show posterior median along with 95% CI for each of 924 individual collectors.

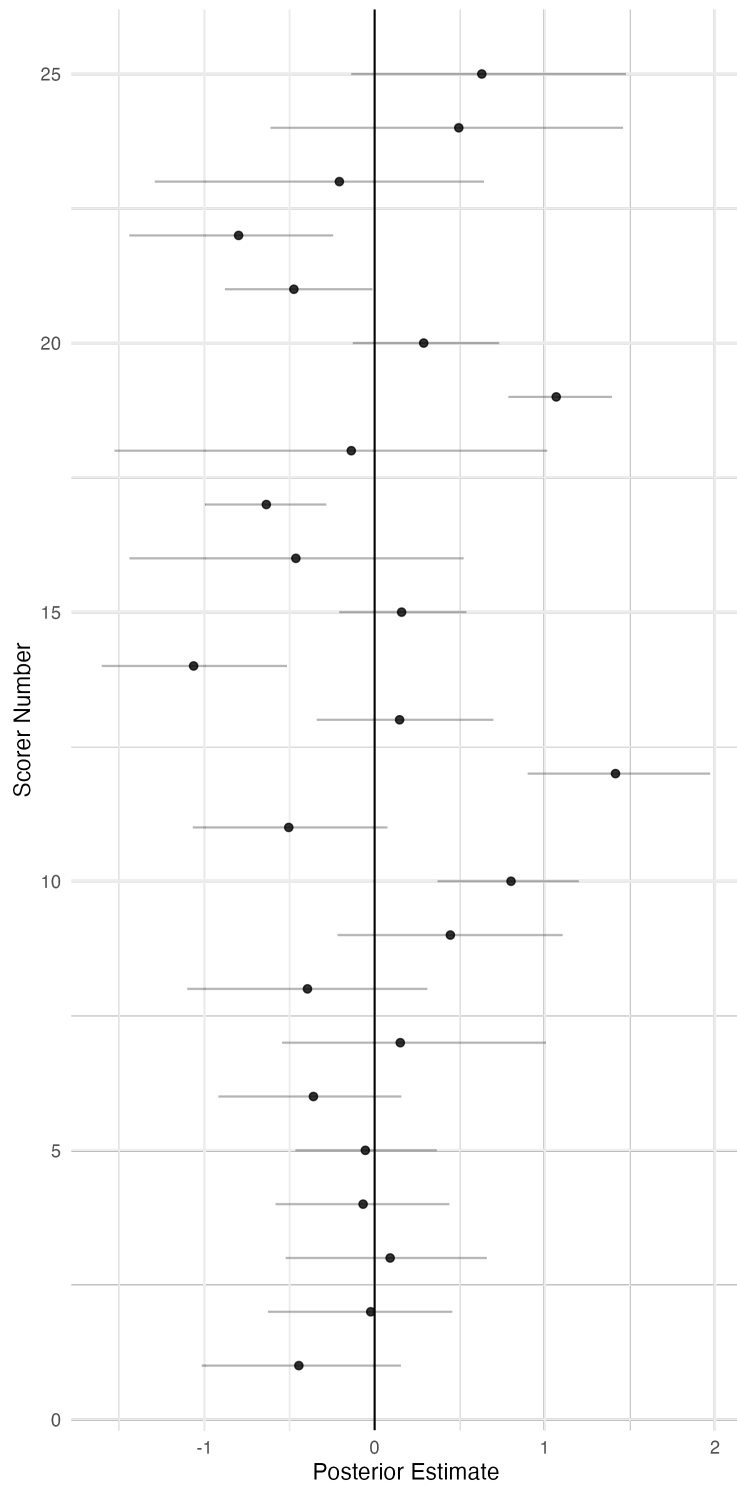


Figure A10: **Posterior estimates of scorer random effects.** Points show posterior median along with 95% CI for each of 25 individual collectors.

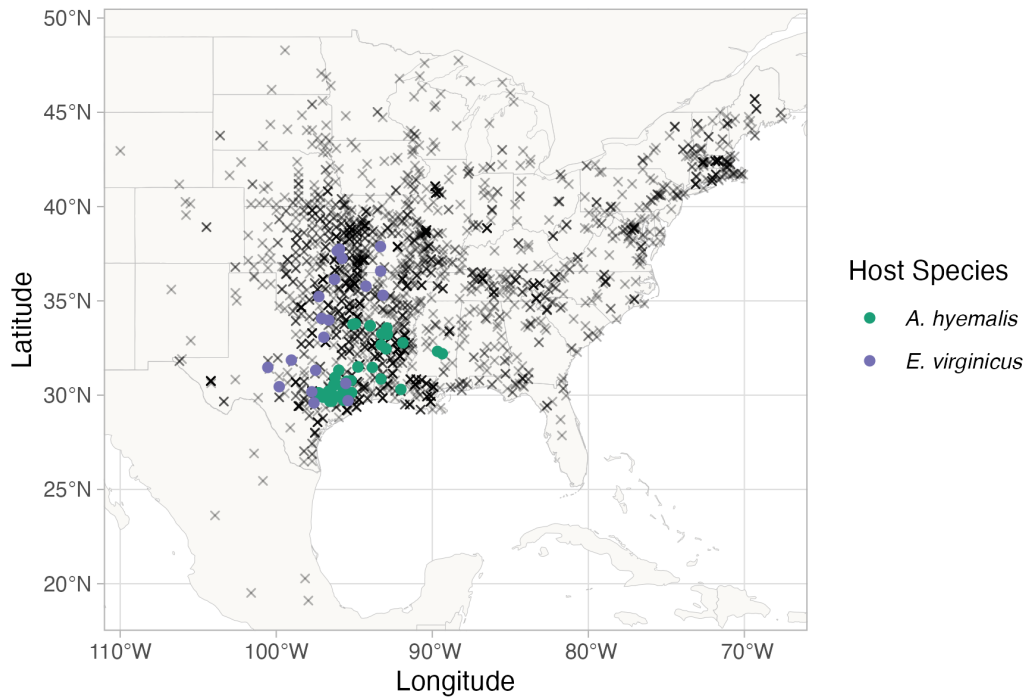
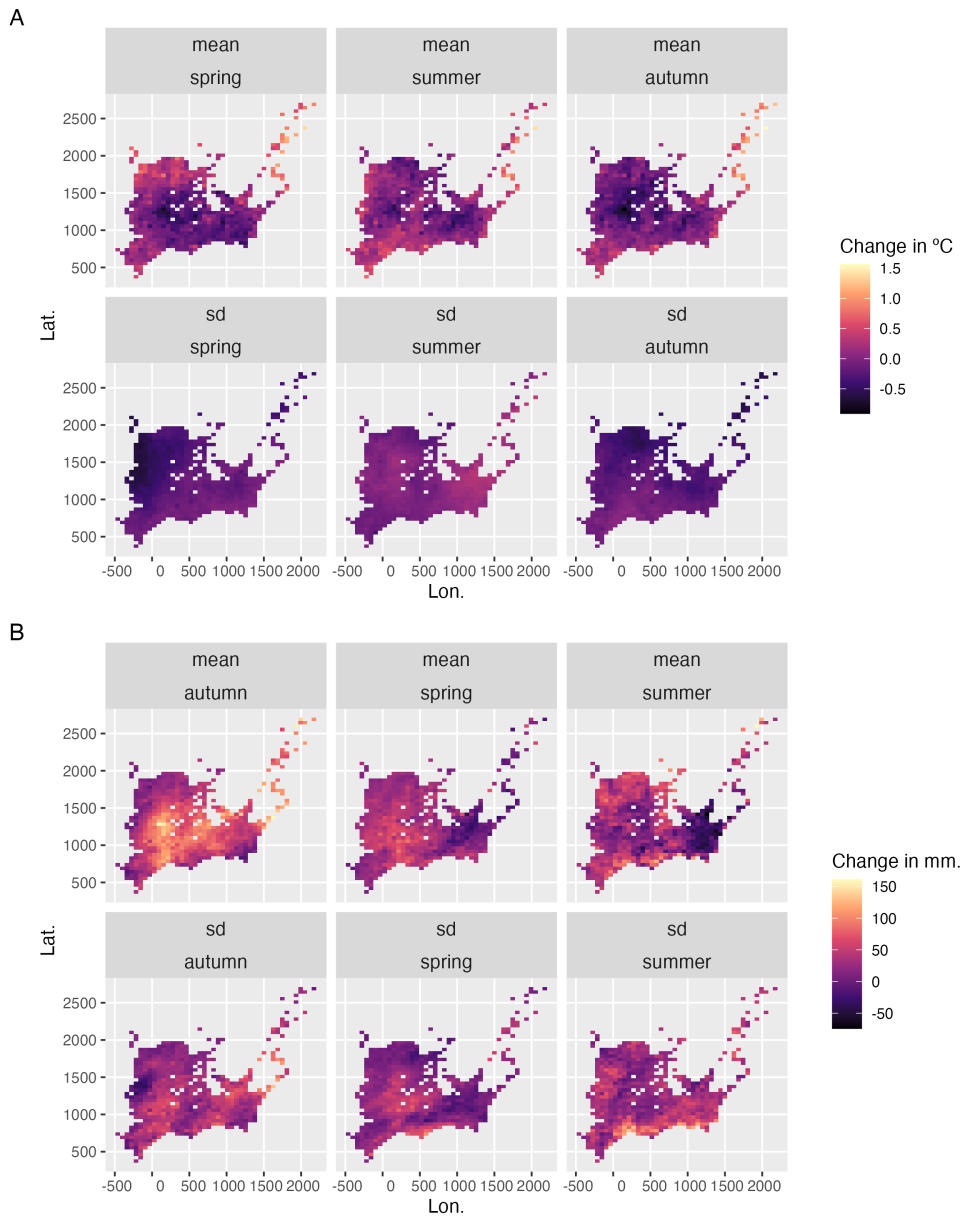
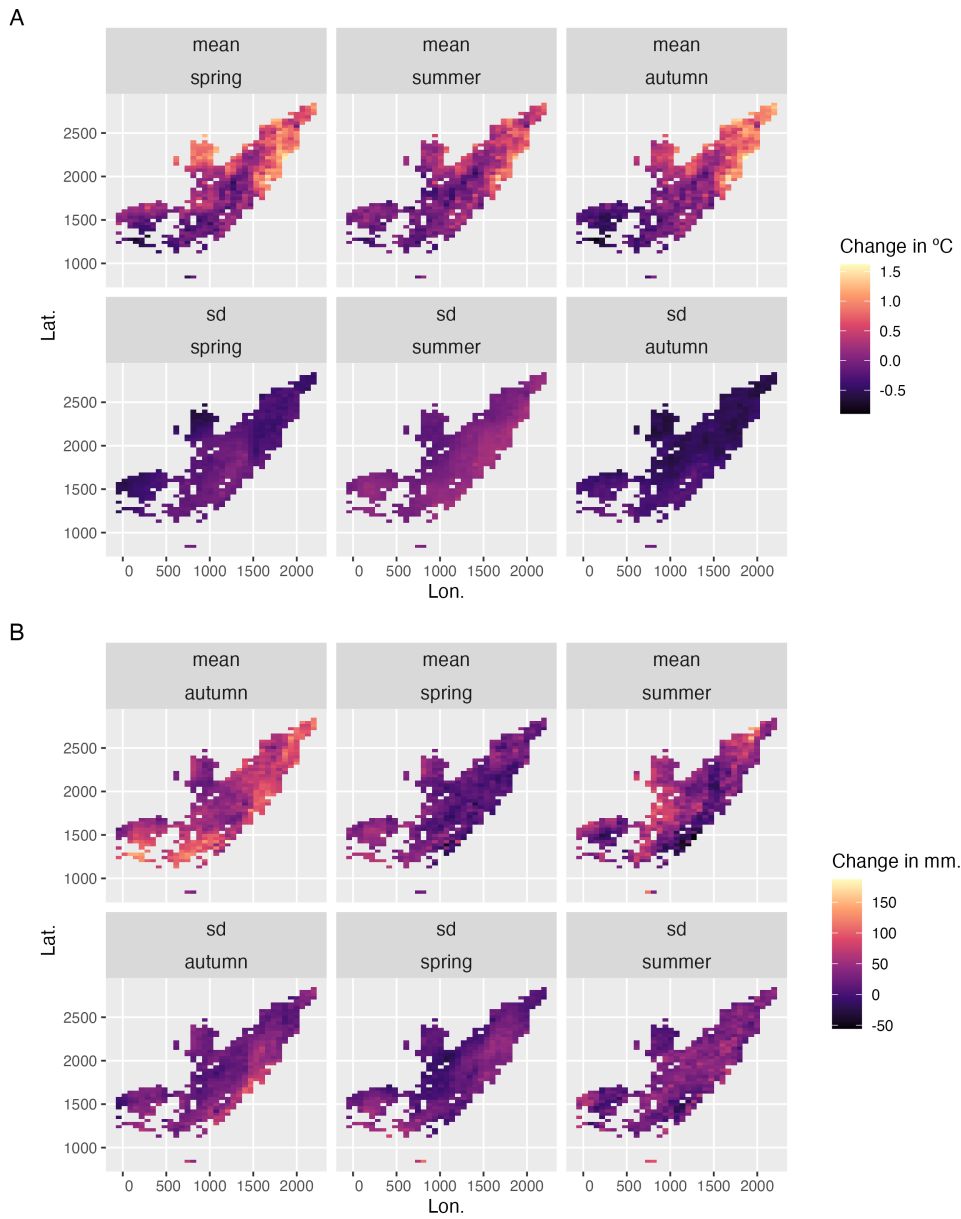


Figure A11: Locations of contemporary surveys of endophytes in *A. hyemalis* used as "test" data (red points), relative to the historical collection data (black crosses).



**Figure A12: Change in seasonal climate variables between the periods 1895-1925 and 1990-2020.** Color represents change in (A) seasonal temperature and (B) seasonal precipitation. Maps show pixels covering the modeled distribution of *A. hyemalis* used in post-hoc climate correlation analysis.



**Figure A13: Change in seasonal climate variables between the periods 1895-1925 and 1990-2020.**

Color represents change in (A) seasonal temperature and (B) seasonal precipitation. Maps show pixels covering the modeled distribution of *A. perennans* used in post-hoc climate correlation analysis.

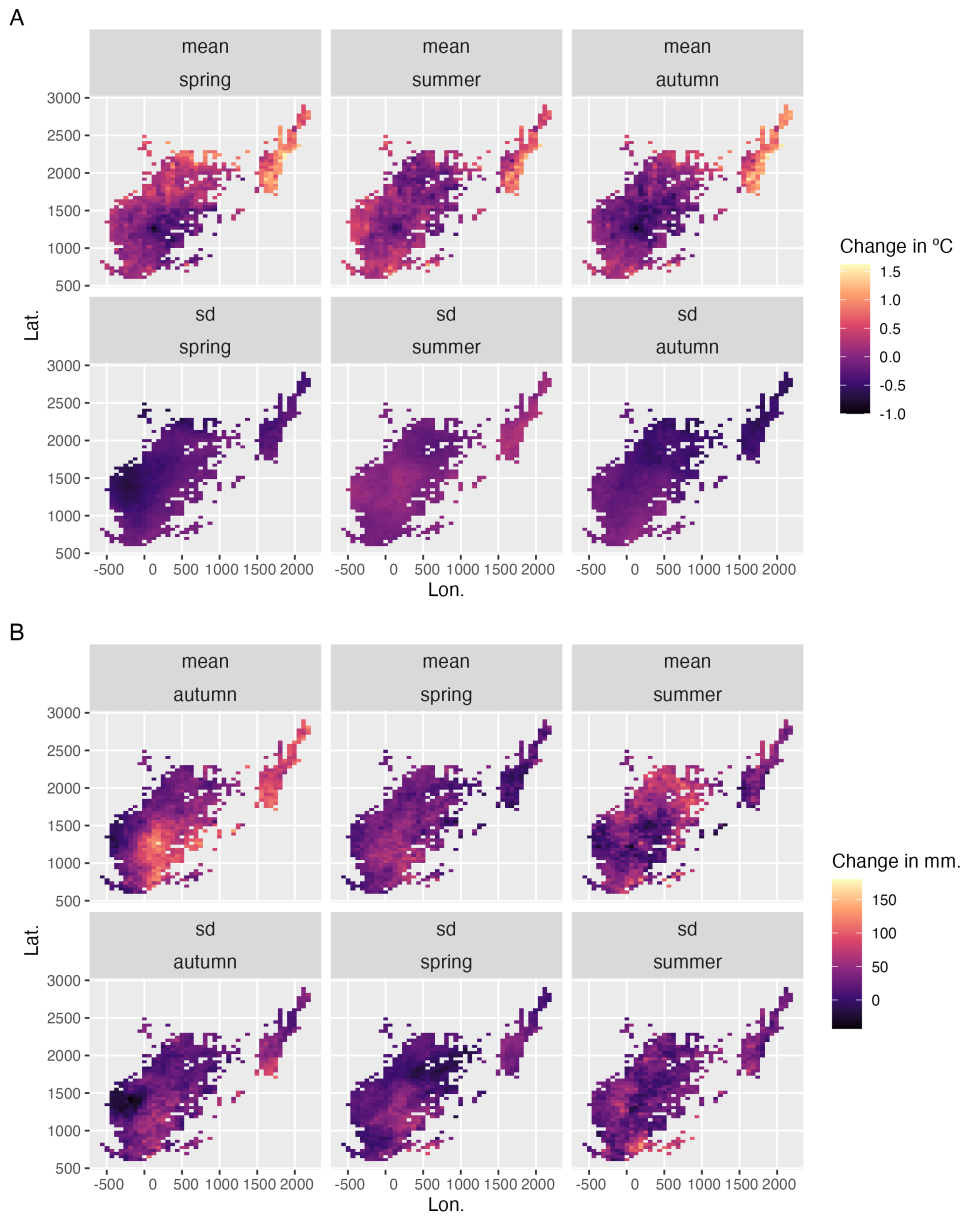


**Figure A14: Change in seasonal climate variables between the periods 1895-1925 and 1990-2020.** Color represents change in (A) seasonal temperature and (B) seasonal precipitation. Maps show pixels covering the modeled distribution of *E. virginicus* used in post-hoc climate correlation analysis.

Table A1: Summary of herbarium samples across collections

Herbarium Collection	AGHY	AGPE	ELVI
Botanical Research Institute of Texas	350	190	198
Louisiana State University	72	38	62
Mercer Botanic Garden	3	–	6
Missouri Botanic Garden	210	205	122
Texas A&M	100	–	72
University of Kansas	134	34	197
University of Oklahoma	85	34	95
University of Texas & Lundell	183	91	102
Oklahoma State University	51	10	74

## Supporting Methods

811

### ODMAP Protocol

#### 813 Overview

814 **Model purpose:** Mapping current distribution of *Epichloë* host species.

815 **Target species:** *Agrostis hyemalis*, *Agrostis perennans*, and *Elymus virginicus*.

816 **Study area:** Eastern North America

817 **Spatial extent:** -125.0208, -66.47917, 24.0625, 49.9375 (xmin, xmax, ymin, ymax).

818 **Spatial resolution:** 0.04166667, 0.04166667 (x, y).

819 **Temporal extent:** 1990 to 2020.

820 **Boundary:** Natural.

#### 821 Data

822 **Observation type:** Occurrence records from Global Biodiversity Information Facility and

823 herbarium collection across eastern North America. We used 713 occurrences records for

824 *Agrostis hyemalis*, 656 occurrence records for *Agrostis perennans* and 2338 for *Elymus virginicus*.

825 **Response data type:** occurrence record, presence-only.

826 **Coordinate reference system:** WGS84 coordinate reference system (EPSG:4326 code)

827 **Climatic data:** raster data extracted from PRISM

828 **Model**

829 **Model assumption:** We assumed that the target species are at equilibrium with their environment.

831 **Algorithms:** Maximum entropy (maxent)

832 **Workflow:** We described the workflow in the method section of the manuscript.

833 **Software:** All statistics were performed using Maxent 3.3.4 and R4.3.1 with packages terra,  
834 usdm, spThin and dismo.

835 **Code availability:** Available through this link: <https://github.com/joshuacfowler/EndoHerbarium>

836 **Data availability:** Will be available upon acceptance

837 **Assessment**

838 We used AUC to test model performance.

839 **Prediction**

840 We predicted the probability of presence of the host species as a binary maps (presence or  
841 absence)

## 842 *Mesh and Prior Sensitivity analysis*

843 To test the influence that the triangulation mesh and choice of priors has on results, we compared  
844 model results across a range of meshes and priors. We re-ran our model for the mesh used in  
845 main body of the text (Fig. A2), which we refer to as the "standard mesh", and with a mesh with  
846 smaller minimum vertices (finer mesh). Finer scale meshes increase computation time. For each  
847 of these meshes, we ran the model with a range of priors defining the spatial range of our spatial  
848 random effects: 342km (the prior used for presented results), as well as ranges five times smaller  
849 (68 km) and five times larger (1714 km). We found generally that these choices did not alter the

850 direction of model predictions, but did influence the associated uncertainty and magnitude of  
851 some effects.

852 For overall temporal trends, we found that models with differing priors predicted consistently  
853 positive relationships over time (Fig. A15).

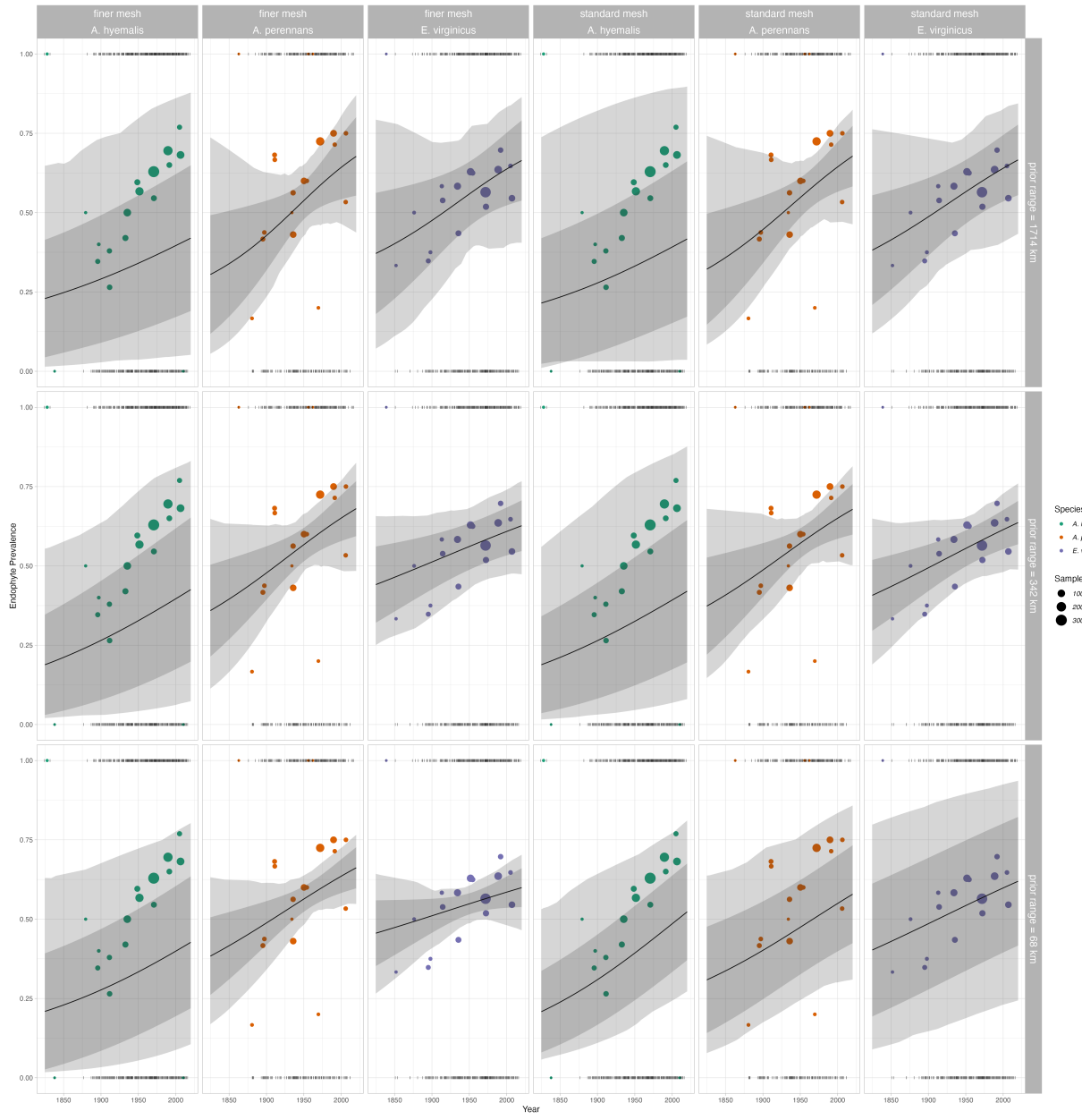


**Figure A15: Overall trend in endophyte prevalence evaluated for models with different range priors on spatially structured random effects, and for two different meshes.** Note that these plots, as compared to Fig. 2 in main text, show mean trends and do not incorporate prediction uncertainty associated with collector and scorer random effects.

854 For spatially-varying temporal trends, we found that models with different priors predicted

855 consistent spatial patterns in temporal trends, although the range of this prediction varied de-  
856 pending on the prior and mesh (Fig. A16 - A17). One noteworthy result of this analysis is that  
857 combinations of prior choice and mesh can introduce instability in model fitting. This is evident  
858 in A16 panel B and A17 panel B, where the prior range is smaller than the minimum vertex  
859 length of the mesh. Model fitting takes an extended time period and the model struggles to  
860 identify variation across space. Results with a set of prior ranges (Fig. A16 - A and C; Fig. A17  
861 - A and C) result in models that estimate trends across space of the same direction and order of  
862 magnitude, although the "smoothness" of these predictions vary.

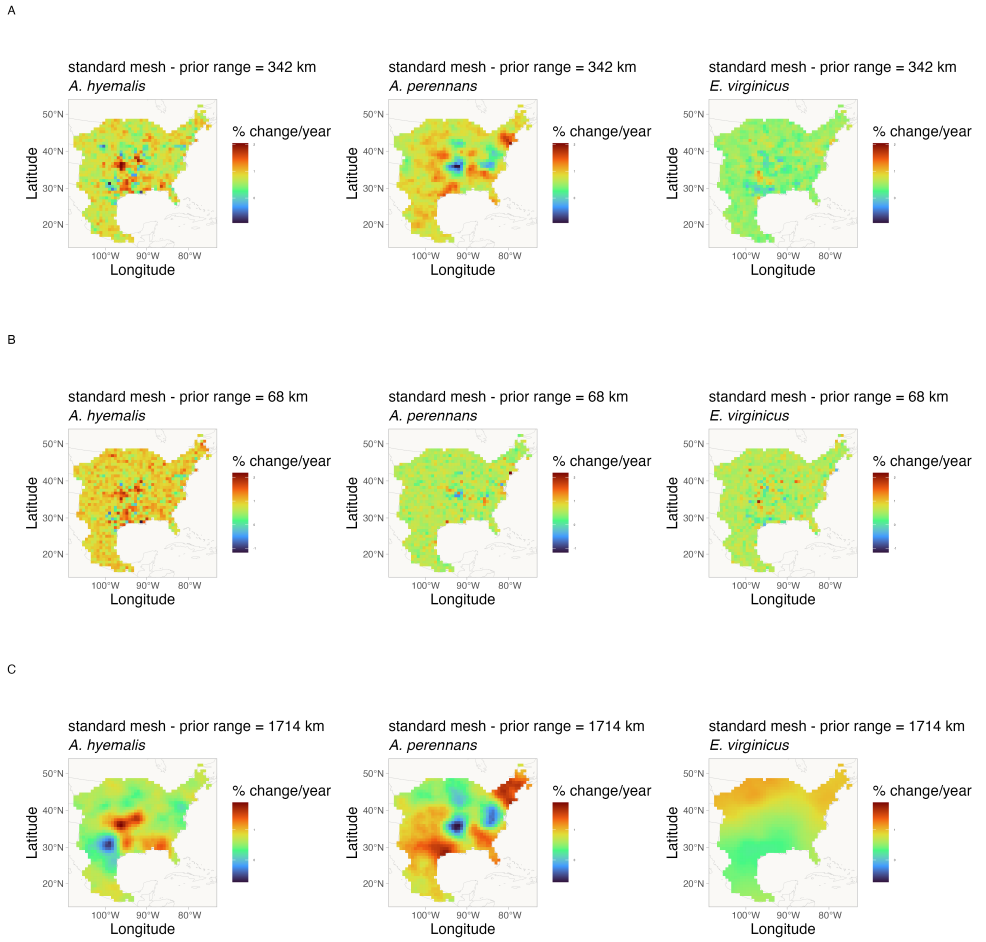


**Figure A16: Spatially-varying trends in endophyte prevalence evaluated for models with different range priors on spatially structured random effects, and for the "standard" mesh.** Shading indicates the magnitude and direction of predicted trends for each of three host species for each of three prior ranges (rows A-C). Note that each plot has an individual scale bars.

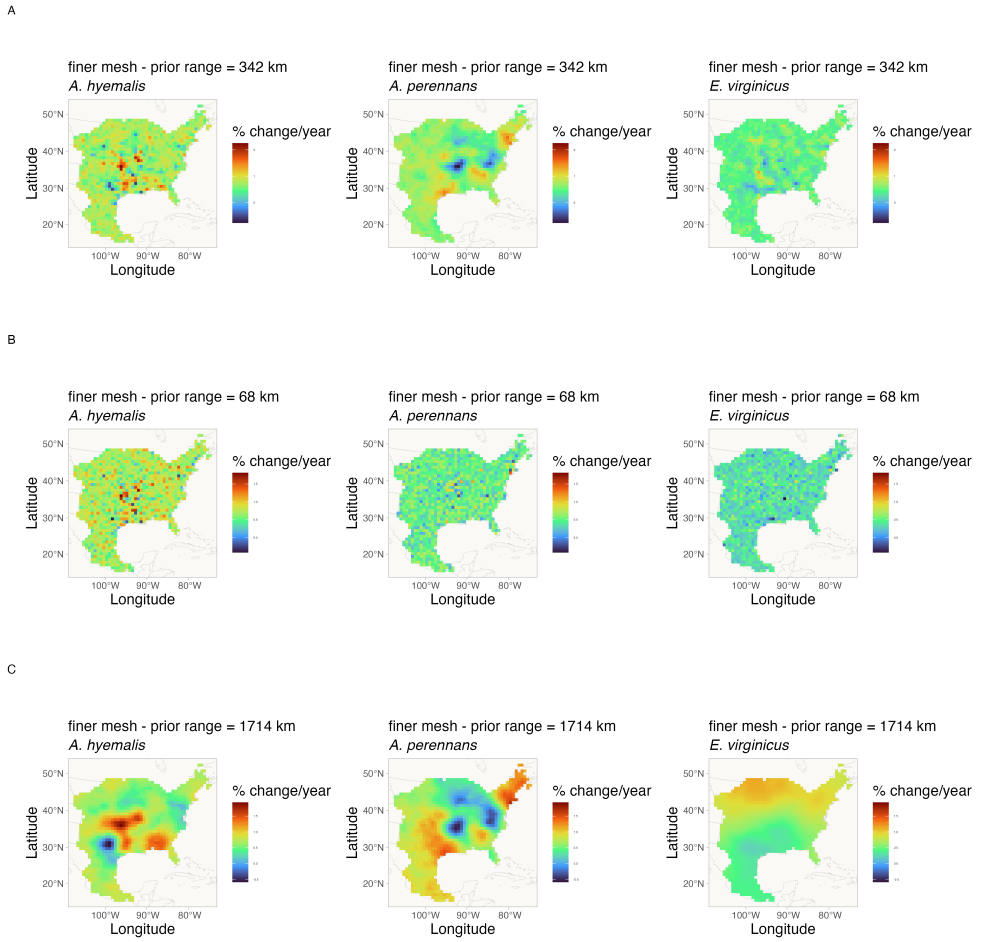


**Figure A17: Spatially-varying trends in endophyte prevalence evaluated for models with different range priors on spatially structured random effects, and for the "finer" mesh.** Shading indicates the magnitude and direction of predicted trends for each of three host species for each of three prior ranges (rows A-C). Note that each plot has an individual scale bars.